Selective modulation of TNF-TNFR signalling for amelioration in experimental autoimmune encephalitis

Iskra Paro
BMS: Neuroscience
Valentina Pegoretti, prof. Ulrich L.M. Eisel
GELIFES-Molecular Neurobiology
University of Groningen
Groningen, 2020

Abstract

Multiple sclerosis is an autoimmune, demyelinating, neurodegenerative disease. One of the prominent targets in modulating the inflammation in MS patients is tumor necrosis factor-α (TNF-α). TNF is a master cytokine involved in maintaining immune system homeostasis in the body but more importantly, increased levels have been correlated with MS in patients. Furthermore, TNF comes in two distinct forms, which bind to two different receptors that have different functions. TNF receptor 1 is involved in pro-inflammatory pathways and activated caspase-mediated cell death. TNF receptor 2 is responsible for cells survival and has been implicated in neuroprotection and immunosuppression via regulatory T cells. Through modulation of both receptors with a TNFR1 antagonist and a TNFR2 agonist, we expect an ameliorated disease course in the mouse model for MS. Analysis of secondary lymphoid tissues and their immune cell compositions will be used to explore the mechanism by which therapeutic effect is achieved. Investigation of different immune cell populations and their movements during the disease state can elucidate new possible targets and also help in explaining the MS immunopathology.

Table of contents:

Introduction

Multiple sclerosis (MS) is an autoimmune, inflammatory and neurodegenerative disease which is currently affecting 2.5 million people around the world. Symptoms can range from sensory and motor aberrations, fatigue and pain to possible cognitive deficits (Dendrou, 2015). The clinical picture among individuals varies significantly mostly because inflammatory lesions develop at different locations along the spinal cord and in the brain. Also, there are several types of MS, delineated by the progression of the disease. Relapse-remitting MS (RRMS) is the most common form of MS. Relapses, increases in inflammation and appearing of focal lesions in the CNS, occur a few times over the span of 8 to 10 years (Howard, 2016). During relapses, the immune cells cross the blood-brain barrier (BBB) and causi it to become more permeable. Immune cells accumulate in the CNS and cluster in localized areas which causes focal lesioning. Lesions are filled with macrophages, B and T cells, plasma cells, neutrophils and pro-inflammatory cytokines and chemokines (Trapp, 2008). The highly pro-inflammatory environment additionally activates resident macrophages (microglia) and drives demyelination, axonal loss and neurodegeneration forming lesions (Compston, 2008). During relapse, the lesions are inactive, and a degree of remyelination and repair can occur. Remyelination in MS leads to improvements in neurologic functioning (Baakilini, 2019). After the initial RRMS, patients slowly transition to the secondary progressive type of MS (SPMS), where the damage to the CNS is irreparable and the disease progresses without recovery periods (Trapp, 2008). Around 15% of patients experience a primary progressive form of MS where there are no initial relapse-remitting periods, the disease is progressive and detrimental from the beginning (Trapp, 2008).

The causing event for the cascade of inflammation, demyelination, axonal loss, synaptic damage and neurodegeneration is still unknown. Immune cells that are attracted to the CNS are activated for self-myelin proteins, but whether this is the first step in MS etiology is still up for debate (Howard, 2016). For now, therapies for MS involve medications reducing symptom severity or immunomodulatory therapies which try to delay the progression by suppressing inflammation (Fletcher, 2010; Howard, 2016).

In search of possible treatment targets, analysis of lesions, cerebrospinal fluids (CSF) and sera of MS patients, showed, among other findings, an elevated level of tumor necrosis factor α (TNF-α) presence (Sharief and Hentges, 1991). TNF-α is a master cytokine, involved in maintaining immune system homeostasis in normal and inflammatory conditions (Probert, 2015) Interestingly, increased TNF-α level was correlated with MS disease severity (Sharief and Hentges, 1991). However, an attempt of anti-TNF therapy in MS patients resulted in exacerbations of the disease (The Lenercept study, 1999). This unexpected failure was soon attributed to the fact that TNF exists in two different forms soluble TNF (solTNF) and transmembrane TNF (tmTNF) which bind to two distinct receptors, TNF receptor 1 (TNFR1) and TNF receptor 2 (TNFR2). TNFR1 is expressed ubiquitously on various cells throughout the body and acts through caspase-mediated apoptosis mechanisms or stimulates the production of pro-inflammatory cytokines such as IL-17 (Ya, 2018). TNFR2 is expressed mostly in immune and epithelial cells and it promotes cell survival through the Pi3K-AKt/PKB signalling and NF-κB activation (Dong, 2015). Studies modulating TNFR1 and TNFR2 individually have shown some promising results. Increased TNFR1 signalling has been directly linked to increasing demyelination and therefore, disease severity in an animal model for MS such as experimental autoimmune encephalomyelitis (EAE) (Eugster, 1999). The EAE model consists of inducing spinal chord inflammation by activating peripheral T cells to be myelin reactive (Constantinescu, 2011). Suppression of TNFR1 signalling in the

EAE model via antagonistic activity has been shown to decrease disease severity (Williams, 2014; Williams, 2018). TNFR2 knock-out animals experienced exacerbated EAE disease course suggesting TNFR2 has a protective role. Agonistic activity on TNFR2 led to neuroprotection and overall lower disease severity (Dong, 2016; Fischer, 2018). Due to the pleiotropic nature of TNF and most opposing effects of the two TNFRs, activity of these two receptors must be balanced and modulated in order to yield beneficial effects. TNF-based therapies are currently used for many inflammatory conditions like Crohn's disease or rheumatoid arthritis, but there are no approved treatments modulating TNF-α signalling for MS (Kaltsonoudis, 2014).

Both EAE and MS pathologies are reliant on immune cell behaviour. Activated T cells cross the blood-brain barrier (BBB) which further destabilizes its permeability, allowing macrophages/monocytes, B cells and more T cells to infiltrate the CNS more easily (Constantinescu, 2011). In EAE, emphasis is put on T cells, specifically T helper CD4+ cells (Th) which are responsible for disease progression and are abundant in lesions. In MS, lesions are filled with macrophages, B cells and more cytotoxic CD8+ T cells than CD4+ cells (Kaer, 2019). Nevertheless, specific CD4+ T cell subsets have been implicated in both EAE and MS, especially since EAE is a CD4+ T cell-mediated inflammatory disease. Th cells secreting interferon γ (IFNγ) or Th1 cells and Th cells secreting interleukin 17 (IL-17) or Th17 cells have both been confirmed to be pathogenic in both EAE and MS (Kaskow, 2018). However, over the years Th17 cells crystallized as more important pathogenic drivers as they significantly propagate the pro-inflammatory environment. Th cells that secrete interleukin 4 (IL-4) or Th2 cells are often of antithetic function compared to Th1 cells and are considered to be anti-inflammatory (Paintlia, 2006). Furthermore, regulatory CD4+ T cells (Tregs) maintain autoimmunity and are involved in supressing long-lasting inflammation. T regs became of special value in TNF-related research, as it was established Tregs express high levels of TNFR2 which can be modulated to expand this protective population (Chen, 2007) and have a protective effect on inflammatory diseases (Fischer, 2018).

With this study we aim to investigate whether a human TNFR1 antagonist, human TNFR2 agonist and their combination can have ameliorating effects on EAE disease progression in humanized mice. The combination of treatments is expected to be more effective in reducing the clinical scores of EAE animals and rescuing body weight loss. By analyzing immune cell phenotypes in the spleen and lymph nodes we will explore whether the treatment effect is modulated by the peripheral lymphoid system. Important immune cell populations such as regulatory T cells (Tregs) and T helper subsets (Th) will be screened for treatment related effects, which could help substantiate overall treatment effect. Further confirmation of neuroprotection in the CNS will be performed by histological analysis of the brain and spinal cord (not a part of this project).

Materials & Methods

2.1. Animals

Female mice aged between 11 to 12 weeks were used in this study. Two transgenic lines, a humanized TNFR1 knock-in (ki) and humanized TNFR2ki with a C57BL6 background (for detailed mouse line description see Dong, 2016) were cross-bred until a double transgenic homozygous line was established and sustained for three generations. Extracellular parts of the TNFR 1 and 2 were humaniyed while the intracellular parts of the receptors were murine.

The animals were housed in standard cages (3-5 per cage). The standard light/dark cycle of 12/12h was used and they had *ad libitum* access to standard food pellet and water. The animal experiment was done in accordance with the European legislation for animal testing (IvD 15360-04-007).

2.2. EAE immunization and observation

When the double transgenic KI mice were 11 to 12 weeks old, they were subjected to the EAE induction protocol. The materials and protocols were obtained from the Hooke lab website (https://hookelabs.com/products/EK-2110/). The Hooke lab kits contained the MOG35-55 antigen in Complete Freund's adjuvant (CFA) and pertussis toxin (PTX) vials. PTX dose was adjusted in a previous experiment to induce a milder EAE course.

Under isoflurane anaesthesia, animals were injected with the MOG35-55 emulsion at two sites along the spinal cord. After the initial immunization, on the same day, they were injected intraperitoneally (IP) with PTX (70ng/injection), and 24h after they were injected with it again. For the next 5 days the animals were left undisturbed in order, to allow the disease to develop and reduce stress.

From the 6th day post immunization (dpi) to the 25th dpi, the animals were scored and weighed everyday around the same time. Scoring was done based on the Hooke lab protocol, where animals are given scores from 0 to 5 relating to their clinical symptoms and ascending paralysis (summarized in Appendix 1). The researcher scoring the animals was blinded to the treatment that the animal was receiving for the sake of unbiased scoring.

2.3. Special animal care

Due to the increasingly severe nature of EAE with time, precautions were taken to alleviate symptoms and also reduce stress experience. Stress can cause EAE to develop irregularly or not at all.

At disease onset the animals were provided with heating mats to help with the pain. Special wet food and hydrogels were provided in the cage to be more accessible and easier to consume for paralyzed and docile animals. Special water nozzles with longer nipples were also provided, as another source of water. All procedures were done in the room where the animals were housed in order to avoid stress from transport. Furthermore, animals were in the same room since the breeding. When the paralysis was significant, some bedding was removed from cages to ease reaching the food and water in the cage.

2.4. Treatment administration

ATROSAB, a TNFR1 antagonist was found to be highly protective in EAE studies (Williams, 2014; Williams 2018). For this study ATROSIMAB was used, which is a newer variant of ATROSAB (Richter, 2019). ATROSIMAB is a human monovalent anti-TNFR1 antibody fragment. Compared to ATROSAB, the variable domains of the heavy and light

chains were fused to N-termini of heterodimerizing Fc chains. This increased the half-life of ATROSIMAB and its binding affinity for TNFR1.

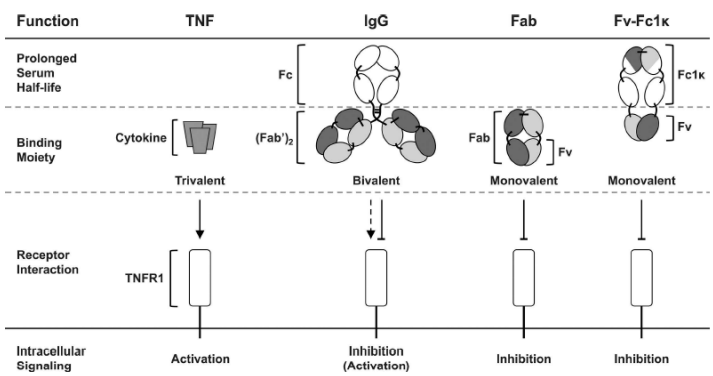

Figure 1. (A) Schematic representation of TNF, IgG ATROSAB, Fab and ATROSIMAB and their comparison in binding, receptor interaction and half-life. Source: Richter, 2019.

For modulating TNFR2 function, an agonist called EHD2-scTNFR2 (EHD2) was used. This is a human TNFR2-selective TNF mutein which binds to the humanized receptors in the mouse (Dong, 2016; Fischer, 2018). The compound consists of a TNFR2-selective single-chain mouse TNF which is fused to a EH-domain-containing protein 2 dimerization domain sourced from the heavy chain CH2 of IgE, making a disulfide-bonded dimer.

Figure 2. Schematic representation of EHD2-sc-TNFR2. Source: Fischer, 2018.

The EAE animals were divided into four groups: EHD2 treatment group, ATROSIMAB treatment group, EHD2+ ATROSIMAB combination treatment group and phosphate-buffered saline (PBS) group as a control (Table 1). The EHD2 treatment group received an IP injection of EHD2 at 6, 9 and 12 dpi. The ATROSIMAB treatment group received an IP. ATROSIMAB injection at 12, 15 and 18 dpi. The combination treatment group received EHD2 at 6, 9 and 12 dpi and ATROSIMAB at 12, 15 and 18 dpi. The control group was injected with PBS at 6, 9, 12 ,15 and 18 dpi. PBS was also given to treatment groups, when they were not receiving the treatment (grey in Table 1). All animals were injected a total of 5 times. Animals were randomly assigned to their treatment group before the start of the study. To avoid bias, treatment injections were prepared by a different researcher than the researcher performing the scoring.

Treatment:	dpi 6	dpi 9	dpi 12	dpi 15	dpi 18
EHD2 o					
ATROSIMAB o					
EHD2+ATROSIMAB					
PBS o					

Table 1. Schematic representation of the treatment plan for this study. Red colour designates treatment with EHD2, blue colour designates ATROSIMAB and the grey designates vehicle injections of PBS.

2.5. Sacrifice and organ collection

The four abovementioned treatment groups (Table 1) were subdivided, also prior to the beginning of this study, into 2 groups based on day of sacrifice. On 18 dpi (acute group) a predetermined number of animals was sacrificed with pentobarbital and 4% paraformaldehyde (PFA) perfusion to study effects of the treatment during the peak of the disease. On 25 dpi (chronic group) the rest of the animals were sacrificed in the same manner. Before perfusing with PFA, spleens and lymph nodes were collected for the FACS staining and put in Roswell Park Memorial Institute medium+ glutamate+ penicillin/streptomycin (RPMI+glu+P/S) in Falcon tubes and stored on ice. After perfusion with PFA, brain, spinal cord, liver and kidney were collected from each animal and post-fixed in 4% PFA overnight. The organs were then washed with PBS and stored for further histopathological analysis. Tip of the tails were also collected for additional genotype confirmation. Blood was collected before immunization via tail vein cut (max 50ul/animal) and before sacrifice with cardiac puncture. The blood samples were then centrifuged (2000g x 10min) and serum was collected for further protein analysis.

2.6. Immune cell isolation from spleens and lymph nodes

Spleens and lymph nodes were strained through 70µm filters to make single cell suspensions in the same Falcon tubes. The suspension of each individual spleen was centrifuged at 1200 rpm for 10 mins. The pellet was treated with 0.83% ammonium chloride and incubated for 4 mins while continuously being shaken. The Falcon tubes were quenched with RPMI+glu+P/S, centrifuged again at 1200 rpm for 10 mins. The pellet was resuspended in fresh media and centrifuged again. Lastly, the pellet was resuspended in RPMI+glu+P/S+ 10% fetal bovine serum (FBS). The cells were counted after diluting 1/25 (2x1/5) in Trypan Blue. The lymph node suspensions were centrifuged at 1200 rpm for 10 mins and the pellet was resuspended again in RMPI+glu+P/S+10%FBS. The cells were counted after diluting 1/5 in Trypan Blue. After counting, around 10^6 cells/organ/well were transferred into U-bottom 96-well plates.

2.7. Flow cytometry staining for cells in suspension

Intracellular stimulation was performed in the U-bottom 96-well plate with 20ng/ml of phorbol myristate acetate (PMA), 1µg/mL of ionomycin and 2µg/mL of Golgiplug. the plate was incubated for 4 hours at 37 ˚C. Cells were transferred to a V-bottom 96-well plate, centrifuged and the supernatant was discarded. The pellets were resuspended in 200uL PBS, centrifuged and the supernatant was discarded again. 100µL of diluted (1/1000 in PBS) Zombie stain was added and incubated for 15 mins in the dark, at room temperature. The plate was centrifuged and the pellet was washed in FACS buffer (washing step).

For blocking of the Fc receptors, each pellet was resuspended in 10% rat serum and incubated for 15mins in the dark at 4˚C. The cells were washed again with 150µL of FACS buffer.

For the extracellular staining the cells were resuspended in FACS buffer with other stains (FIT-C, BV610, BV510, Pacific Blue, Alexa Fluor 700, PerCP/Cy5, BV786) and incubated for 15 mins in the dark at room temperature. After the washing step, the cells were centrifuged again and the supernatant needs to be flipped off.

For the intracellular staining, the pellet needs to be resuspended in 200µL Nucleofix/Nucleoperm™ and incubated for 30 mins in the dark at 4 ˚C. The pellets are then washed with 200µL of Perm/Wash™ each, centrifuged and the supernatant is flipped off. The

pellets are resuspended in 100µL of P/W buffer with belonging stains (PE/Dazzle, PE/Cy7, PE-A, Alexa Fluor 647) and incubated for 15 mins in the dark at room temperature. The cells are washed with 150µL P/W buffer, then washed again with 200µL P/W and finally resuspended in 200µL FACS buffer.

The cells were stored on ice and sent to Hassel University (Belgium) tobe analyzed by a flow cytometer (FACS Diva). The stains were chosen based on a recommended panel from Hasselt University (Table 2). The .fcs files were sent back for analysis.

Antibody	Antigen	Cells expressing the antigen
Zombie NIR	live/dead	Cells that are dyed are considered dead
Alexa Flour 700	CD45	Leukocytes
PerCP/Cy5.5	CD11b	Monocytes/macrophages/neutrophils
BV785	Ly6C	Migratory monocytes/macrophages
BV650	CD19	B cells
FITC	CD3	T cells
BV510	CD8	Cytotoxic T cells
Pacific Blue	CD4	Helper T cells (Th)
PE-A	IL-4	Th2 cells and natural killer cells (NK)
PE/Dazzle594	IL-17	Th17
PE/Cy7	IFN-γ	Activated T cells and NK
Alexa Flour 647	FoxP3	Regulatory T cells

Table 2. Panel for flow cytometry staining as recommended by the Hasselt University in Belgium.

2.6. Analysis of flow cytometry data

a) Manual gating

Digital .fcs files were uploaded into the FlowJo™ Software (FlowJo Software v10; Becton, Dickinson and Company, 2019) workspace. Analysis was first performed on samples from the spleens and then samples from the lymph nodes, separately. In the workspace the algorithm FlowAI was applied in order to distinguish cells that passed through the flow cytometer properly from those that did not (Monaco, 2016). The algorithm creates the first gate called GoodEvents. All further analysis was done on this gate. Cells were then gated for singlets (FSC-A/FSC-H or FSC-A/FSC-W), live cells (FSC-A/Zombie-NIR) and leukocytes (FSC-A/AF700). Leukocytes were divided into B cells and T cells (CD19/FITC-A). Samples with low numbers (<600) in the T cell gate were excluded from further analysis (Appendix 2). T cells were separated into CD4+ and CD8+ cells (Pacific Blue/BV510). From the CD4+ population, Th1-like cells (CD4+IFNγ+), Th2-like cells (CD4+IL-4+), Th17-like (CD4+IL-17+), and Tregs (CD4+FoxP3+) were distinguished (example of gating can be found in the Appendix 2). Percentages of cells of these populations in respect to the entire CD4+ population and percentages of CD8+ cells within the T cell population were taken for statistical analysis which was performed in GraphPad Prism.

b) FlowSOM

T cell populations from all samples were used for producing FlowSOM trees. FlowSOM is a two-step clustering algorithm (Van Gassen, 2015). First, cells are clustered based on

expression markers recorded by the flow cytometer. Then, populations of cells are metaclustered and visualized on a minimum spanning tree (MST) to show relation between these populations and cells within them. Samples were grouped based on organ, time of sacrifice (acute/chronic group) and treatment. Within each subgroup, the corresponding samples were concatenated, in such a way, that all treatment groups had the same number of cells in the concatenated file. This was done with the DownSample algorithm (FlowJo Software v10; Halpert, 2019) which preserves the distribution of cells across T cell subpopulations but reduces the number of events present. This is a necessary step that allows FlowSOM trees to be compared. A minimum spanning tree (MST) was first generated for a concatenated file that includes cells from one organ, one time-point, but all treatment groups. This file can have a higher number of cells than individual treatment groups. FlowSOM is then run on each concatenated file representing a treatment group. MST trees obtained were compared visually.

2.7. Statistical analysis

Data representing clinical scores, body weight loss, cumulative score and disease onset are presented as mean ± SEM. Statistical significance was tested by the Kruskal- Wallis test and was followed by Mann-Whitney tests for between group comparisons. The figures and statistical analysis were performed in GraphPad Prism. Normality of values was checked in SPSS v26, separately. No outliers were highlighted during the SPSS check. Data representing frequencies of certain immune cell populations are presented as mean± SEM. Normality was checked in SPSS v26 and all populations were normally distributed. Statistical significance was tested with one-way ANOVA and post-hoc Tukey's range test. Significance was determined as $p<0.05$* and $p<0.001$**.

Results

ATROSIMAB, EHD2-scTNFR2 and their combinatory effect ameliorate EAE progression in mice

Humanized ki mice were immunized with EAE and observed daily throughout 18 or 25 days. Their response to different treatments was deduced from clinical scores, body weight changes and day of disease onset. The expected EAE development includes the onset of the disease being between 9 to 14 dpi, followed by the peak of the disease which lasts 3 to 5 days (Hooke Kits™ for EAE induction, 2020). This is usually followed by a partial recovery and another, less severe relapse. All treatment groups reach overall lower scores than the control group (Figure 3, Figure 5). The control group shows a steep increase in score during the onset of the disease, reaching the peak. The increase is less steep for the EHD2 group. Both the ATROSIMAB and combination group experience an even lower increase and reach peak at a lower score. The ATROSIMAB group curve shows a worsening of the symptoms from 22 dpi which increases for the rest of the study. For the combination group, overall clinical scores steadily decrease till 25 dpi, with a slight increase recorded before the sacrifice.

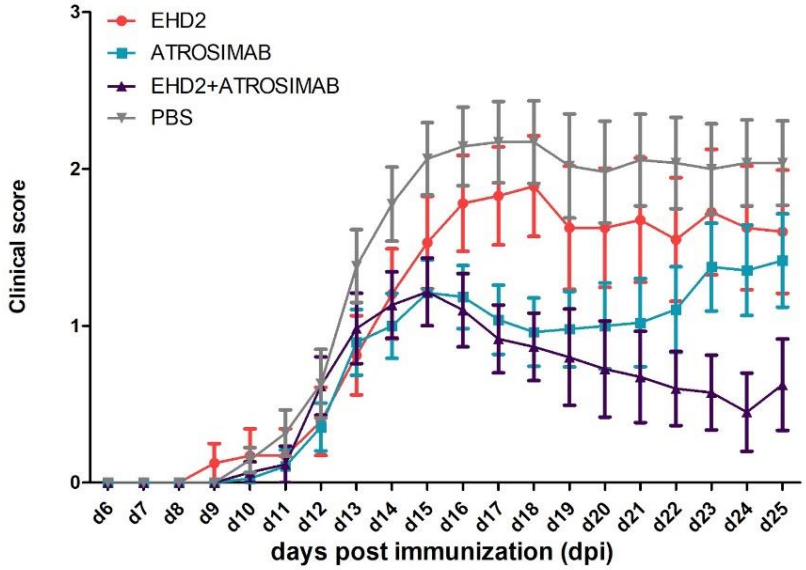

Figure 3. All treatment groups show an ameliorated EAE disease course based on clinical scores. The effect is less pronounced in the EHD2 treatment group. Characteristic peak, recovery and relapse are seen in each curve. The control group received vehicle injections and overall had the highest disease severity Clinical scores per day, per treatment over 25 days are presented as mean ± SEM. Animals that died before the sacrifice days were excluded from the graph and further analysis (see Appendix 4). Animals from both acute and chronic group are represented on the graph.

Treatment effect in the EAE model is usually determined based on cumulative scores reached and disease onset. By comparing cumulative scores of treatment groups from the chronic group, significant differences between both the ATROSIMAB and combination group, and the control can be established. At the acute stage, no differences in cumulative scores were recorded (see Appendix 3), indicating that the treatment effect is not detectable at high levels of inflammation.

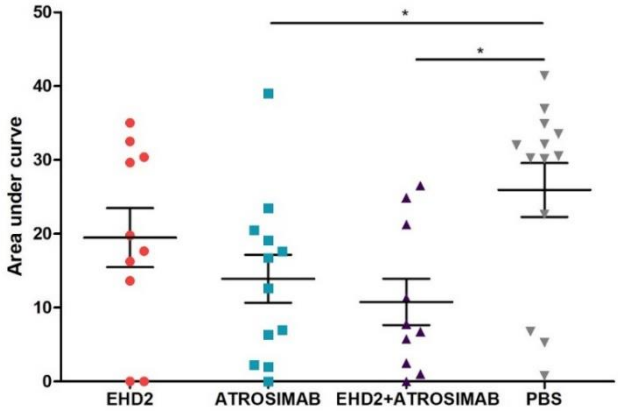

Figure 4. Cumulative EAE score is represented as the area under the disease curve (Figure 1). The ATROSIMAB and combination treatment groups significantly differ in cumulative score achieved during the 25-day observation. The graph shows animals from the chronic group, divided per treatment. Values are presented as mean ± SEM. Kruskal- Wallis test was performed to establish a significant difference between means for all groups. After that, the Man-Whitney test was done for comparison between groups. Significance was noted when p value <0.05*.

Most animals developed disease 13±3 dpi and there were no significant differences in disease onset between groups in the chronic stage. As some animals developed disease after 18 dpi, disease onset and incidence for the acute stage were not included in the results. An expected 10% of animals did not develop EAE, which is in accord with the induction kit's failure rate. However, the chronic EHD2 group's disease incidence is 80%, lower than the others.

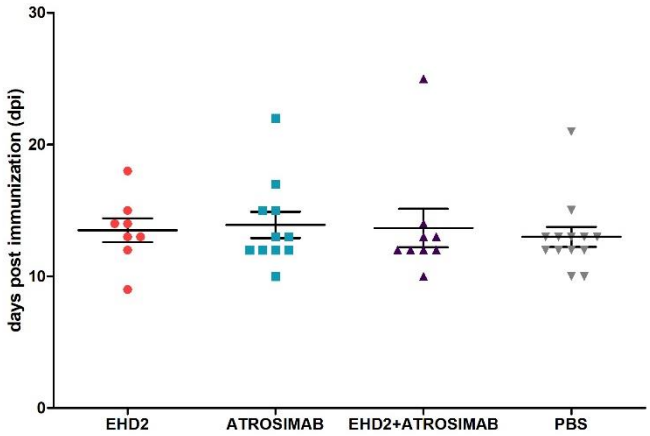

Figure 5. No significant difference was found in disease onset. Animals on the graph are from the chronic group. Day of disease onset is presented as mean± SEM. No significance was detected by Kruskal-Wallis or Man-Whitney tests.

Treatment	n(chronic):	n(animals that did not develop EAE):	Disease incidence:
EHD2	10	2	80%
ATROSIMAB	12	1	91.67%
EHD2+ATROSIMAB	10	1	90%
PBS	13	1	92.3%

Table 3. The disease incidence for the chronic group is represented. The EHD2 group shows decreased disease incidence, while 90% of animals in other groups regularly developed EAE.

Furthermore, disease progression can be assessed through body weight loss. When the animals are experiencing higher scores due to increased symptoms, their body weight usually decreases. In the periods of recovery, the scores decrease, and the body weight increases. After the peak mice slowly gain back some of the weight, even if it does not correspond to the clinical score. The PBS group shows a convincingly highest percent of body weight loss, with the lowest rate of recovery weight gain until the 20th dpi. All treatment groups overall showed a lower rate of weight loss, but the animals in the combination group lost the least weight, when compared to others.

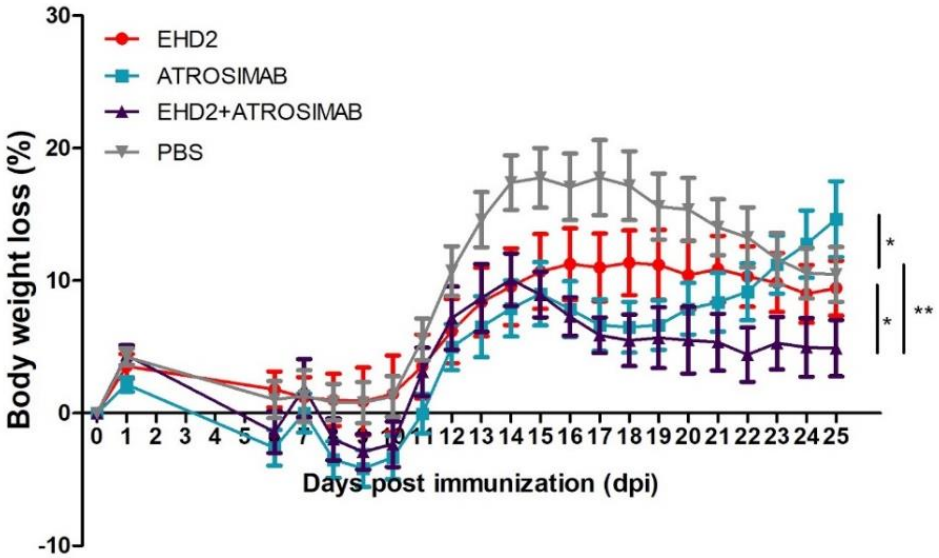

Figure 6. Graph representation of the percentage of body weight loss over a period of 25 days. Animals in the ATROSIMAB and combination treatment group lost less weight than the control. The combination group also was significantly more effective in rescuing body weight loss than the EHD2 group. Body weight was calculated as loss with respect to body weight measured at 0 dpi and is presented as mean ± SEM. Animals represented in this figure belong to the chronic cohort. Kruskal-Wallis test was performed as to check significant differences between means. Afterwards, Mann-Whitney test were applied to compare all groups with each other. These tests were chosen as the data does not follow a normal distribution. Significance was labelled $p< 0.05$* and $p<0.01$**.

On 12 dpi, the EHD2 group received the third injection of EHD2, and the combination group received both EHD2 and ATROSIMAB. Around 25 minutes after they received the third treatment injection, some of the animals started exhibiting shock-like symptoms, like heavy breathing, gasping, convulsions and isolation from other mice in the cage. The mortality rate after the third injection is represented in Table 4.

Treatment	Number of animals in total:	Number of animals that died prematurely:	Mortality rate after third injection:
EHD2	21	5	19.05%
ATROSIMAB	19	0	0%
EHD2+ ATROSIMAB	23	8	30.43%
PBS	21	1	0%

Table 4. Mortality rate after the third injection of animals per treatment group is depicted in the table. 20% of animals in the EHD2 group died and 30% in the combination group. Animals from other groups never died after treatment was administered. Some were found dead or sacrificed due to very high scores and low body weight (see Appendix 4).

Modulation of both TNFR receptors leads to a longer lasting therapeutic effect

EHD2 has been established to have a protective effect on CNS inflammation (Dong, 2016). Furthermore, ATROSAB, a previous variant of ATROSIMAB ameliorates EAE severity in humanized mice (Williams, 2018). Their combinatory effect showed to be longer-lasting than their individual action (Figure 7). Treatment effect on 15 and 18 dpi is visible in all treatment groups, though only ATROSIMAB and combination reach significance. After 25 days, clinical scores of the combination group were still significantly lower than the control, while the therapeutic effect of ATROSIMAB, which was previously also significant, decreased. Animals from both acute and chronic groups are represented, except for the dpi25, where only the chronic group is represented. The combination groups score at 25 dpi was similar to the score from day 18, which was the last treatment day. Hence, seven days after the last intervention, treatment effect is only seen in the combination group, suggesting more consistent effect elicited by the interplay of both compounds.

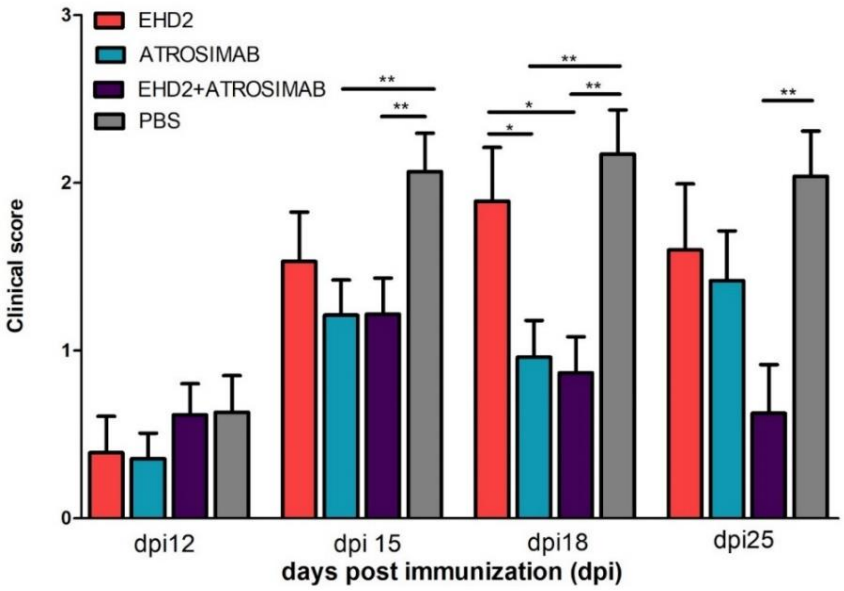

Figure 7. The combination treatment group experiences overall lower clinical scores and for a longer period of time. On treatment day 6, 9 (not pictured) and 12 there are still no significant differences in the clinical scores per treatment. Clinical scores per treatment, per day are presented as mean± SEM. The data did not pass the normality check and was therefore tested with the Kruskal-Wallis test. This was followed by Mann-Whitney tests for comparisons between groups. Significance was labelled *= $p< 0.05$ and **= $p<0.01$.

CD4+ subsets in the spleen and lymph nodes do not mediate therapeutic effect of ATROSIMAB and EHD2-scTNFR2

EAE is a CD4+-mediated inflammatory disease. T helper subsets from the spleens and lymph nodes were observed in an effort to explain if treatment effects are caused by the changes in the immune cell population behaviour in the periphery. Analysis of Th subsets showed no differences between treatment groups, but some trends were observed.

Th1 cells are important pathogenic drivers in EAE (Kaskow, 2018). In the spleen (Figure 8A), during the acute stage, all treatment groups have similar numbers of Th1-like cells. In the chronic stage, higher numbers can be observed, especially in the ATROSIMAB and combination group, which could be treatment related since a lower number of Th1-like cells is present in the EHD2 group. Comparison to the PBS group in this case is unreliable, as the sample size is small and the values are variable. In the lymph nodes (Figure 8B), there is overall a smaller number of Th1-like cells than in the spleen samples, but the trend between the acute and chronic stage is opposite from the trend in the spleen. Higher numbers of Th1-like cells are present in the acute stage, suggesting pro-inflammatory activity, although the numbers vary within treatment group. During the chronic stage, there is around 1% of Th1-like cells in the CD4+ population, but the number is slightly elevated in the combination group.

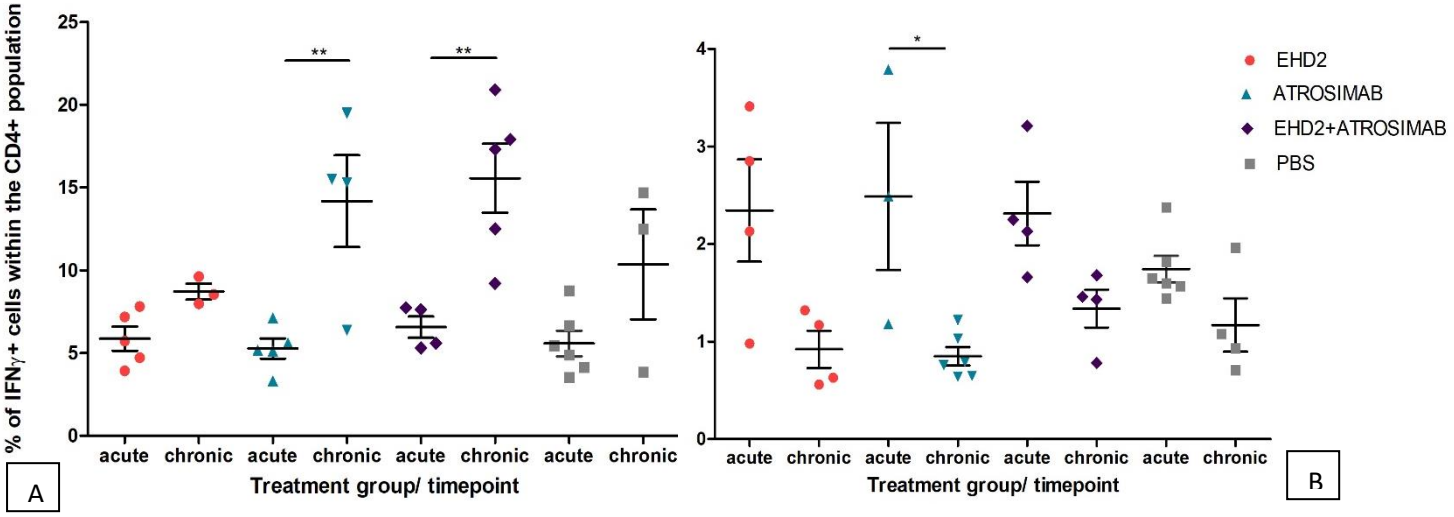

Figure 8. No significant differences in the quantity of the CD4+IFNγ+ population between treatment groups. (A) Represents % of IFNγ+ cells within the CD4+ population in the spleen, across all treatment groups. Significant difference between the acute and chronic stage of the ATROSIMAB and combination group, respectively. (B) Represents % of IFNγ+ cells within the CD4+ population in the lymph nodes, across all treatment groups. Significant difference between the acute and chronic stage of the ATROSIMAB group. One-way ANOVA followed by post-hoc Tukey's range test. Significance was established as $p<0.05$*, $p<0,001$**.

Another CD4+ pathogenic subset are cells secreting IL-17 (Th17-like phenotype) (Maddur, 2012). Similar trends can be observed in the spleen, for both Th1-like and Th17-like cells. There are lower amounts of Th17-like cells in the acute stage and higher amounts during the chronic stage (Figure 9A). However, the differences are not as pronounced as for the Th1-like cells. In the lymph nodes, the percentages of Th-17 like cells are highly variable for both the acute and chronic group, and no trends can reliably be established (Figure 9B).

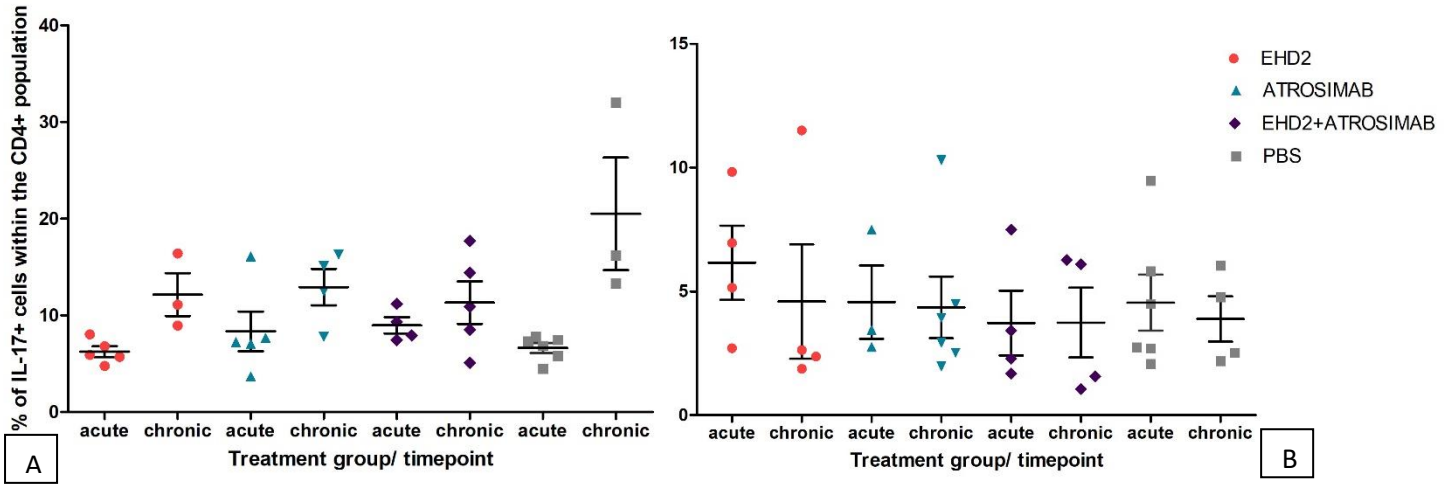

Figure 9. No significant differences in the quantity of the CD4+IL-17+ population between treatment groups. (A) Represents % of IL-17+ cells within the CD4+ population in the spleen, across all treatment groups. (B) Represents % of IL-17+ cells within the CD4+ population in the lymph nodes, across all treatment groups. One-way ANOVA followed by post-hoc Tukey's range test. Significance was established as $p<0.05$*, $p<0{,}001$**.

Th cells that secrete IL-4 (Th2-like phenotype) are considered to be anti-inflammatory (Kaer, 2019). They are present in both spleen and lymph nodes at much higher rates than Th1-like and Th17-like cells. In the spleen (Figure 10A), higher amounts of Th2-like cells are present during the acute stage, and lower amounts during the chronic stage. Samples in the EHD2 group are more variable than in other groups. Amounts of CD4+IL-4+ cells in the lymph nodes (Figure 10B) are the same and consistent in the acute and chronic stage for the combination and control group. However, for the EHD2 acute and ATROSIMAB chronic group, samples vary.

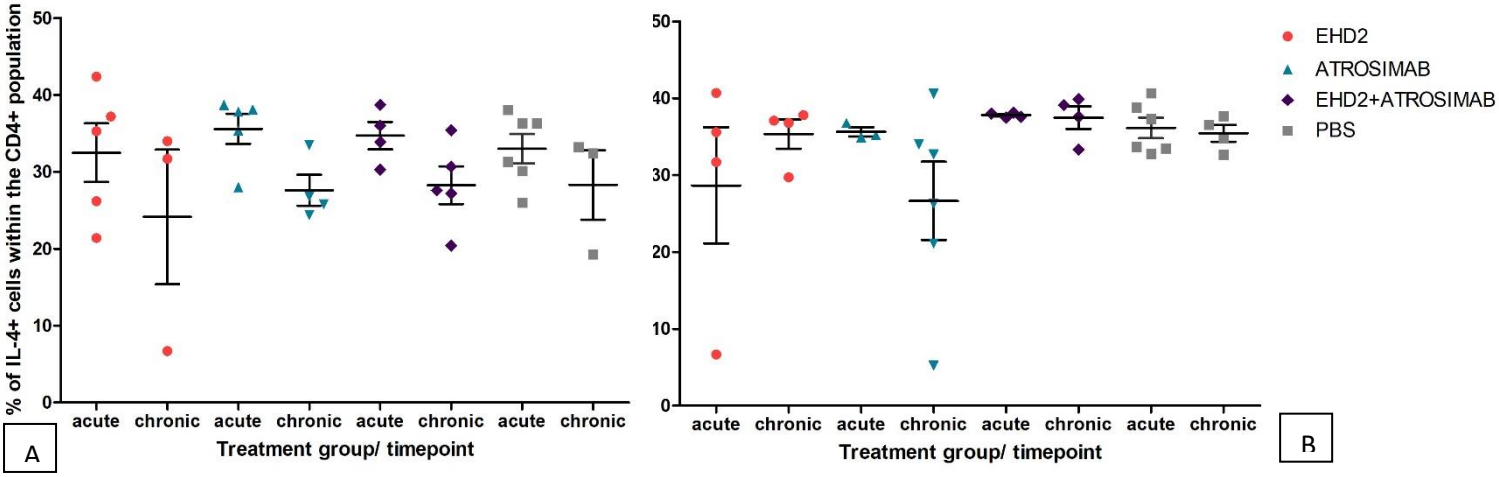

Figure 10. No significant differences in the quantity of the CD4+IL-4+ population between treatment groups. (A) Represents % of IL-4+ cells within the CD4+ population in the spleen, across all treatment groups. (B) Represents % of IL-4+ cells within the CD4+ population in the lymph nodes, across all treatment groups. One-way ANOVA followed by post-hoc Tukey's range test. Significance was established as $p<0.05$*, $p<0{,}001$**.

Regulatory T cells are the bodies mechanism of maintaining autoimmunity, which makes their role in MS highly important. Expansion of these cells has been noted as a response to EHD2 (Fischer, 2018). However, in this study, no significant differences in Treg populations were found in between treatment groups. In the spleen (Figure 11A), lower and consistent

numbers of Tregs are present during the acute stage. During the chronic stage, there is an increase in Tregs for all groups, but the increase is significant for the ATROSIMAB and control group. Groups that were receiving EHD2 did not reach significance. In the lymph nodes, numbers of Tregs within the CD4 population are somewhat similar across all timepoints and treatment groups (Figure 11B).

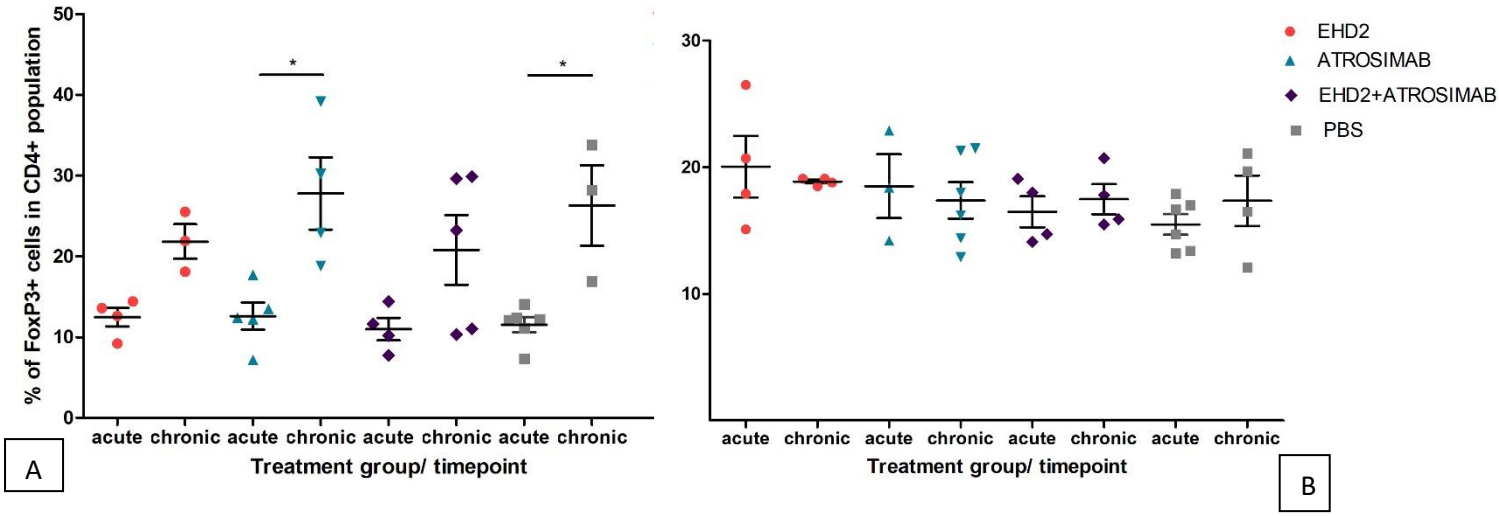

Figure 11. No significant differences in the quantity of the CD4+FoxP3+ population between treatment groups. (A) Represents % of FoxP3+ cells within the CD4+ population in the spleen, across all treatment groups. Significant difference in numbers of Tregs between the ATROSIMAB and the controls acute and chronic stage. (B) Represents % of FoxP3+ cells within the CD4+ population in the lymph nodes, across all treatment groups. One-way ANOVA followed by post-hoc Tukey's range test. Significance was established as $p<0.05$*, $p<0{,}001$**.

Results up until this point were produced by manual gating of populations in FlowJo. Additional information on T cell subset populations and their relations with one another is provided by FlowSOM trees. Two MSTs are shown below, representing FlowSOM results from the spleens of animals from EHD2 treatment group and the ATROSIMAB group at the chronic stage of the disease. The pie chart in figure 12A represents each cell marker applied with a different colour which serves for cell phenotyping. Background colouring of the pie charts on the MST indicates metacluster belonging and size of the cluster represents the abundance of cells within the cluster. All other FlowSOM trees of other treatment groups can be found in Appendix 5.

Clusters with dark blue colouring express two phenotypes: CD4+IFNγ+ and CD4+IFNγ+IL-4+ which are separated on the MST. The CD4+IFNγ+ population can be considered of the Th1-like phenotype and is more abundant in the ATROSIMAB group (Figure 12B) than the EHD2 group (Figure 12A). Populations with purple background colouring correspond to the Th2-like phenotype (CD4+Il-4+). They are more abundant than other cell populations, which confirms results from the manual gating. Interestingly, CD4+IL-17+ cells or the Th17-like phenotype show to be more abundant in the ATROSIMAB group and the PBS group (Appendix 5) than the EHD2 and combination group. This visual difference was not supported by manual gating. Furthermore, the Treg population did not fully separate from the CD4+ population (green colouring) on the MST. The population representing only the CD4+FoxP3+ cells is enclosed in a red rectangle in Figure 12A. When visually comparing,

the EHD2 group shows more of these cells than the ATROSIMAB group. Also, the combination group shows similar amount of CD4+FoxP3+ cells as the ATROSIMAB group and the PBS group shows smaller clusters than all treatment groups.

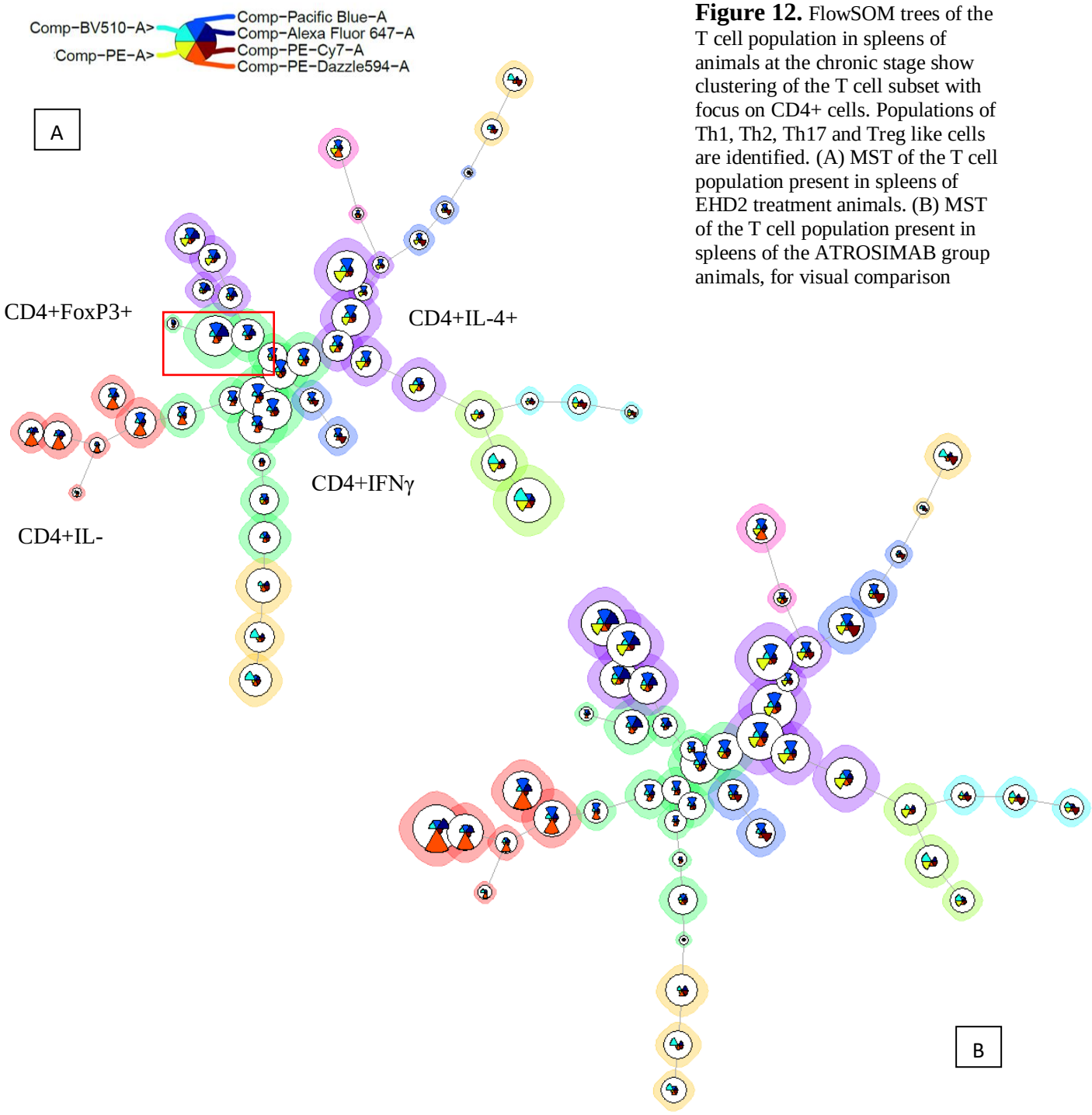

Figure 12. FlowSOM trees of the T cell population in spleens of animals at the chronic stage show clustering of the T cell subset with focus on CD4+ cells. Populations of Th1, Th2, Th17 and Treg like cells are identified. (A) MST of the T cell population present in spleens of EHD2 treatment animals. (B) MST of the T cell population present in spleens of the ATROSIMAB group animals, for visual comparison

Considering EAE is a CD4+ mediated disease, a big part of the disease progression and possible treatment targets are immune cell populations implicated by literature so far. These results show no differences in relevant CD4+ subsets, yet treatment effect is apparent through clinical scores and body weight. Conclusively, CD4+ subsets in the periphery (spleen and lymph nodes) did not mediate the observed therapeutic effect.

CD8+ T cells could have significant role in amelioration of EAE via TNF modulation

CD8+ T cells are considered cytotoxic, pathogenic cells in MS/EAE (Friese, 2009). Research in EAE has often focused on CD4+ cells, while CD8+ cells were left to the side. More significant roles and possible regulatory functions of CD8+ T cells are coming to light in the recent decade (Sinha, 2015). Interestingly, CD4+ cells were the target population of this study, but the CD8+ population crystallized as the one with treatment related differences (Figure 13A). In the spleen, the combination group had a significantly higher number of CD8+ cells than the EHD2 group at the acute stage. This suggests that the ATROSIMAB in the combination group could be the reason for this boosting effect. The ATROSIMAB group also had relatively more CD8+ T cells at the acute stage than the EHD2, but their numbers are comparable to the control. The increase in the combination group could be due to the combinatory approach. In the chronic stage, the EHD2 group had relatively more CD8+ cells than in the acute stage, whereas all other groups had less cells in the chronic stage. Furhermore, the ATROSIMAB and PBS groups had a similar, consistent number of CD8+ cells at the chronic stage, and this number is lower than the amount of cells in the EHD2 and combination groups. Groups receiving EHD2 also had more variability between samples. In the lymph nodes (Figure 13B), less CD8+ cells were present at the acute stage than the chronic stage across all treatments, but the difference was bigger in treatment groups receiving EHD2, and less pronounced in the ATROSIMAB and control group. These results would suggest that there is an effect of EHD2 on the CD8+ T cell population at the acute stage.

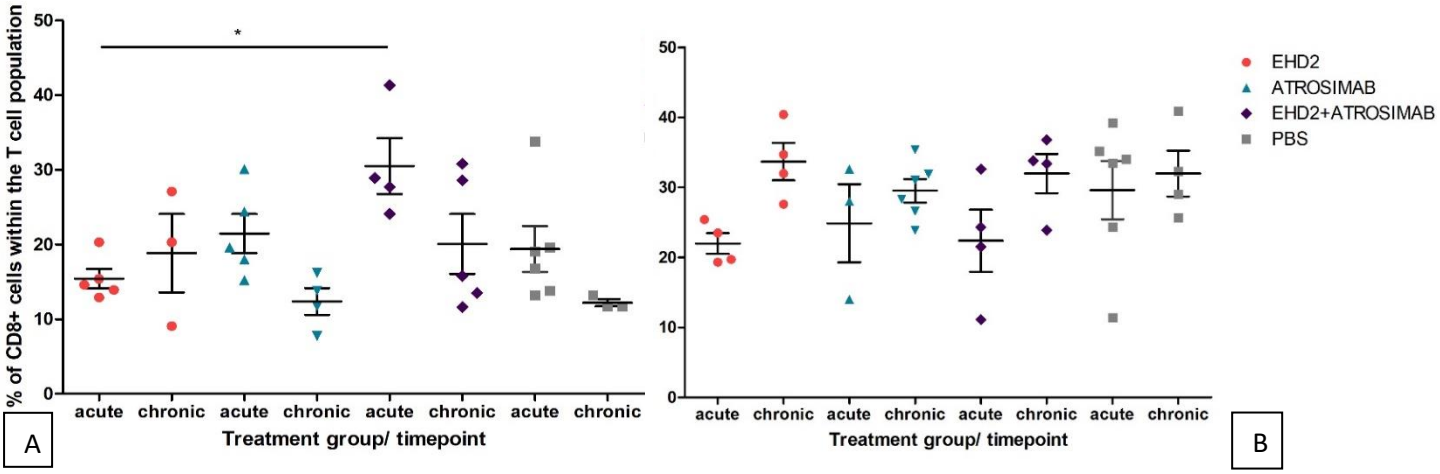

Figure 13. The amount of CD8+ T cells in the spleens of the combination group is significantly higher than in the EHD2 group, at the acute stage. No other significant differences in the quantity of the CD8+ populations between treatment groups. (A) Represents % of CD8+ cells within the T cell population in the spleen, across all treatment groups. (B) Represents % of CD8+ cells within the T cell population in the lymph nodes, across all treatment groups. One-way ANOVA followed by post-hoc Tukey's range test. Significance was established as $p<0.05$*, $p<0,001$**.

Automatic clustering of the cells done by the algorithm FlowSOM further corroborated differences in CD8+ T cell population in response to different treatments. Two MSTs are shown below, representing FlowSOM results from the spleens of animals from combination treatment group and the control group at the acute stage of the disease. Based on metacluster colouring, two distinct populations of CD8+ T cells can be observed. On the Figure 13A they are encapsulated by red rectangles. The metaclusters with red background coloring consist of CD8+IL-4+ cells. In the combination group, this population is expanded. The yellow

population represents CD8+IFNγ+ (Figure 14A, left) and CD8+ cells (Figure 14B, right). Although metaclustering suggests common affiliation, these populations are separated on the MST. When visually comparing these trees, the CD8+ cells are more abundant in the combination group than in the control group and other treatment groups (see Appendix 5).

Higher number of CD8+ cells was established by manual gating as well, but important distinctions between CD8+ cell subpopulations are elucidated by the FlowSOM. These distinctions indicate the role of CD8+ T cells in the periphery might be involved in the therapeutic effect in this study.

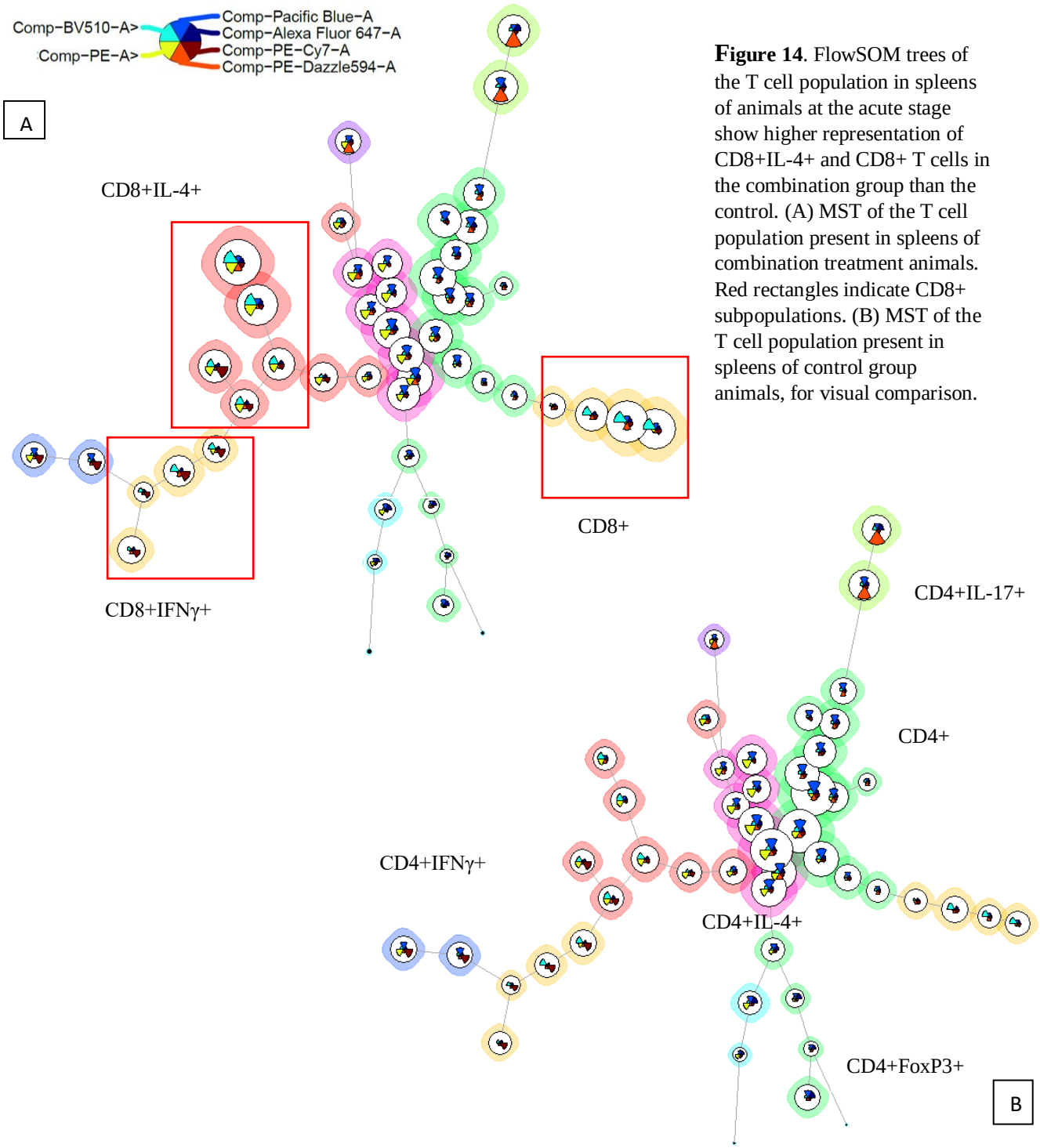

Figure 14. FlowSOM trees of the T cell population in spleens of animals at the acute stage show higher representation of CD8+IL-4+ and CD8+ T cells in the combination group than the control. (A) MST of the T cell population present in spleens of combination treatment animals. Red rectangles indicate CD8+ subpopulations. (B) MST of the T cell population present in spleens of control group animals, for visual comparison.

Discussion

Administration of EHD2-scTNFR2 and ATROSIMAB individually and their combination ameliorated EAE progression in humanized, double KI mice. The treatment effect was observed in the sum of daily disease scores over 25 days. We showed a drop in the cumulative scores in the treatment groups and a longer-lasting ameliorated effect in the combination treatment group, which confirms selective modulation of TNF- TNFR signalling as a better approach to TNF based therapy. Furthermore, body weight loss is also a following indicator of treatment effect and can usually be correlated to clinical scores in EAE (EAE Induction by Active Immunization in C57BL/6 Mice, 2019). While the correlation was not tested in this project, the drop in body weight in treatment groups corresponds to the increase in scores during the peak of the disease. Also, a drop in body weight is observed once again in the ATROSIMAB group corresponding to the scores increase at the end of the study.

The ATROSIMAB group experienced a relapse (Figure 3), which can even be argued to be the peak of the disease for this group. The severe nature of the relapse could indicate that the ATROSIMAB effect was suddenly abrupted. The half-life of the compound is 41 ± 18h (Richter, 2019), which is longer than ATROSAB. However, animals receiving ATROSAB experienced ameliorated scores till day 24 dpi, with their last injection being at 12 dpi (Williams, 2018). The treatment was effective for 12 days after the last injection and the relapse was less severe. In this study, the treatment was effective for 4 days after the last injection. In both studies the compound was given therapeutically, although in the ATROSAB study four injections were given and in this study three were administered. ATROSIMAB effect could be affected by an anti-drug response. Repeated administration of monoclonal antibody compounds can lead to decreased therapeutic efficiency due to formation of anti-drug-antibodies (ADAs) (Vaisman-Mentesh, 2019). ADAs can interfere with the treatment binding to its target receptor and ADA levels were positively correlated to increasing clinical scores in the ATROSAB study (Williams, 2018). Faster and steeper relapse of animals receiving ATROSIMAB could be due to a more potent anti-drug response.

The obvious difference in disease courses between the ATROSIMAB and combination groups is the effect of EHD2. Yet, due to the limited number of days for observation (till 25dpi), whether the combination group would have also gone through a steep relapse, but with a slight delay, is up for exploration. On day 25dpi a slight increase in scores is recorded for the combination group, which is a possible indication that even with EHD2 administration beforehand, ATROSIMAB would cause ADA formation. A follow-up project with a longer duration is warranted. Additionally, increased mortality due to EHD2 injections should be further explored and addressed. Out of all animals receiving EHD2, 30% died after the third injection (Table 4). Animals that died exhibited shock-like symptoms indicating an adverse reaction to the treatment. The cause of this reaction is unknown, but the event has happened in previous studies within this research group. A possible explanation could lie in the fact that, although the humanized compounds target humanized receptors, the reaction takes place in the mouse body. In addition, IL-4 is a cytokine usually involved in allergy responses, and FlowSOM trees highlighted high production of IL-4 by both CD4+ and CD8+ cells (Killestein, 2003), further suggesting anaphylaxis. In addition, no correlation was established between mice that died due to the injection and their clinical scores.

The human EHD2 compound variant (EHD2-scTNFR2) was used in humanized EAE mice and showed a protective effect. So far, the human variant was used in a humanized model for neurotoxicity (Dong, 2016), and mouse variant (EHD2-sc-mTNFR2) in EAE (Fischer, 2019). While therapeutic effect was recorded in both treatment groups receiving EHD2, the effect in this study was smaller than expected in the EHD2 group. It could be that the EHD2-scTNFR2 in humanized mice produces a less protective effect via Tregs than the mouse EHD2 in non-humanized mice (Fischer, 2019). However, an effect was definitively observed, especially when looking at the clinical score development in the combination group (Figure 7). Furthermore, the difference in the long-term response of the ATROSIMAB and combination groups highlights the therapeutic effect of EHD2. The relative half-life of EHD2 is 16.5 hours (Fischer, 2018), yet the ameliorating effect on scores of the combination receiving group was present till 25 dpi. This suggests a priming process that occurred between 6 to 12 dpi, before most animals developed symptoms. Additionally, the priming effect being more prominent in the combination group further substantiates the need for selective modulation of both receptors. Based on the flow cytometry results from the periphery, this pre-emptive protection probably occurred within the CNS, but this will later be confirmed by histological results (not a part of this project).

Heavy accent in TNF-related therapy research is put on Tregs of the CD4+FoxP3+ phenotype. Regulatory T cells supress development of autoimmune diseases and dampen inflammatory responses (Chen, 2007). These cells consistently express TNFR2 at higher levels than effector T cells. When stimulated, TNFR2 activates expansion and stabilization of the Treg population in both the spleen and the CNS (Chen, 2007; Yang, 2018). Furthermore, the mouse variant of EHD2-sc-mTNFR2 has been shown to cause the Treg expansion in mice (Fischer, 2019). The expansive effect ultimately leads to more Tregs being available to suppress detrimental inflammation. Additionally, Tregs can inhibit IL-17 production and decrease the amount of Th17 cells that are differentiating (Miller, 2015). No significant expansion of Tregs or decrease in Th17 cells was observed in this study. This could be related to the EHD2-scTNFR2 effect in humanized mice. Although Tregs have been found to be suppressive in EAE in mice, in humans their suppressive effect was shown to be decreased under TNF modulation (Nie, 2016) Another issue to be considered is the FACS panel set-up could also be the reason for this inconclusive result. FoxP3 is a well-established marker for Tregs, especially CD4+FoxP3+ cells, but Tregs are more often characterized by an additional marker for CD25+ (Chen, 2010). Moreover, FoxP3 can also be found on effector T cells (Chakraborty, 2017). therefore following-up on these results with the addition of the marker for CD25 expression would be insightful. Furthermore, even though there was no significant delay in disease on-set, animals receiving EHD2 did have a lower disease incidence (Table 3), which could indicate EHD2 might have a restorative effect on Treg dysregulation. This effect could be a result of a priming mechanism on Tregs, as EHD2 was given prophylactically, before symptom on-set (Nie, 2016).

For better interpretation in future research, FACS results from the periphery should be compared to CNS immune cell composition. This way, correlations between the populations and their movements could be drawn. Another way to better investigate spleen and lymph node populations would be the addition of markers for distinction between effector or memory cells within the organ. A study by Alvarez- Sanchez et al. in 2015 distinguished the T cell subset of EAE animas by T effector memory, T central memory and naïve T cells by

marking CD44 and CD62L.The spleen is usually a site of both generation and degradation of immune cells. The inguinal lymph nodes are generally a draining compartment, but lymph nodes are also a site for expansion of immune cells. Moreover, in vivo tracing of immune cells could also be a useful tool in elucidating pathogenic and immunosuppressive populations and their movements during disease development and progression (Lee, 2016). Distinction between populations being generated to drive pro- or anti-inflammatory mechanisms or populations being flushed out of the CNS could be of value for understanding EAE pathology under TNF modulation.

Analysis of immune cell compositions in the spleen and inguinal lymph nodes at both the acute and chronic stages resulted in no treatment related differences. Since EAE is a CD4+ mediated disease and CD4+ cells are responsible for triggering the inflammatory cascade in EAE (Lassman, 2017), analysis of the CD4+ subset was of interest. In MS, Th1 cells initiate spinal chord inflammation, while Th17 cells also infiltrate the brain stem, cerebellum and the brain (Hemmer, 2015). Concurrent with MS, Th1 and Th17 cells have been recognized to have pathogenic roles in EAE (Thakker, 2007; Barthelemes, 2016). In regard to MS, Th1 cells play a smaller role than Th17 cells in EAE (tHart, 2011). CD4+IFNγ+ cells are responsible for the initial development of EAE (Thakker, 2007). These cells enable Th17 cells to enter the CNS (O'Connor, 2008). Once Th17 and Th1 cells are in the CNS, they activate resident microglia and induce new cells to differentiate to effector phenotypes (Kaskow, 2018). Deletion of IFNγ can enhance EAE severity, supporting the view that, although they are important in EAE development, they are not the main pathogenic force (Kaskow, 2018). Th17 cells secrete IL-17 which is a highly pro-inflammatory cytokine. IL-17 plays a major role in recruiting all other types of immune cells in the CNS which maintains and drives inflammation (O'Conner, 2008, Thakker, 2007). Higher proliferation and storage of both pathogenic phenotypes would have been expected in the control group, yet this effect is not seen in the periphery. At the chronic stage in the spleen, there is an increase in CD4+IFNγ+ cells in the ATROSIMAB and combination group when compared to the two other groups. However, the control group is variable and represents only 3 animals, which makes the attribution of this effect to ATROSIMAB or EHD2 impossible. Also, the study using ATROSAB on humanized mice found no treatment-related differences in the numbers of Th1 cells (Williams, 2018). Th2 cells are differentiated with the help of IL-4, which they continue to secrete in their maturity. IL-4 can interfere with the differentiation of Th1 cells, making them beneficial in EAE (Kaer, 2019). Therefore, an increase in their numbers as a response to treatment would have been desirable.

While the treatment effect was not modulated by peripheral CD4+ T cells, significant differences were found in the peripheral CD8+ T cell population even without concurrent CNS comparisons. In MS lesions they outnumber CD4+ T cells, and oligoclonal bands can be found at the site of pathology (Sinha, 2015). EAE can be induced with CD8+ MOG-specific cells, confirming their pathogenic role in EAE. At the same time, depletion of CD8+ cells caused an exacerbation in the EAE disease course which suggests an immunosuppressive function (Balashov, 1995; Sinha, 2015). Indeed, CD8+ cells can have regulatory effects that lead to immunosuppression in inflammatory diseases (Gravano, 2013). In this study, CD8+ populations discerned by the FlowSOM algorithm can be described as CD8+, CD8+IFNγ and CD8+IL-4+. Under the CD8+ umbrella, these cells showed a response to treatment. However, this response cannot reliably be categorized as pathogenic or

immunosuppressive. There is an increase in CD8+ T cells in the combination group, yet this group showed a meaningful treatment effect. Even at the chronic stage, both groups receiving EHD2 show, higher, although variable, CD8+ cell numbers in the spleen. Proper phenotyping of this population and better understanding of CD8+ cells in EAE could elucidate whether these CD8+ cells in the spleen are regulatory or effector populations and whether they are being expanded for transport to the CNS or are in the spleen to be degraded. Further flow cytometry experiments could elucidate CD8+ population behaviour, if results from the periphery and CNS along different time-points would be paired. Moreover, IFNγ producing CD8+ cells are cytotoxic in function, but conflicting reports of these cells contributing to recovery and subduing of inflammation exist (Balashov, 1995; Whitacre, 2004). IFNγ CD8+ cells usually have specific targets which are subjected to cytotoxic action leading to target elimination. Under TNFα modulation, encephalitogenic CD4+ T cells can become new targets for these cells, resulting in a decrease of pro-inflammatory processes (Sinha, 2015). This would be a step closer in explaining the expansion of this subpopulation in the combination group (the expansion is also seen in the ATROSIMAB tree, see Appendix 2). Interestingly, CD8+IL-4+ cells are rarely associated with MS or EAE. These cells were found to be regulatory in patients of ankylosing spondylitis, an inflammatory disease of the spine, and their numbers were higher in healthy controls (Zhang, 2009). Moreover, one study showed that stimulation of activated CD4+ and CD8+ cells with MOG35-55 did increase the numbers of both CD8+IFNγ+ and CD8+IL-4+ cells within 24-48h in vitro (Peng, 2019). This effect should be confirmed in vivo with a longer observation period.

To conclude, selective modulation of TNFR1 and TNFR2 leads to an ameliorated EAE disease course with potential to be translated to human MS conditions. Further exploration in the EHD2 priming effect on Tregs and the potency of ATROSIMABs' anti-drug response is warranted. Moreover, exploration of CD8+ populations and their regulatory potential under TNF modulation could open up new targets for manipulation and lead to sooner clinical investigations.

Bibliography:

1. Álvarez-Sánchez N, Cruz-Chamorro I, López-González A, Utrilla JC, Fernández-Santos JM, Martínez-López A, Lardone PJ, Guerrero JM, Carrillo-Vico A.(2015) Melatonin controls experimental autoimmune encephalomyelitis by altering the T effector/regulatory balance. *Brain Behav Immun*. Nov;50:101-114.
2. Baaklini CS, Rawji KS, Duncan GJ, Ho MFS, Plemel JR.(2019) Central Nervous System Remyelination: Roles of Glia and Innate Immune Cells. *Front Mol Neurosci*. Sep 19;12:225.
3. Balashov KE, Khoury SJ, Hafler DA, Weiner HL. (1995) Inhibition of T cell responses by activated human CD8+ T cells is mediated by interferon-gamma and is defective in chronic progressive multiple sclerosis. *J Clin Invest*. Jun;95(6):2711-9.
4. Barthelmes J, Tafferner N, Kurz J, de Bruin N, Parnham MJ, Geisslinger G, Schiffmann S.(2016) Induction of Experimental Autoimmune Encephalomyelitis in Mice and Evaluation of the Disease-dependent Distribution of Immune Cells in Various Tissues. *J Vis Exp*. May 8;(111):53933.
5. Chen X, Bäumel M, Männel DN, Howard OM, Oppenheim JJ.(2007) Interaction of TNF with TNF receptor type 2 promotes expansion and function of mouse CD4+CD25+ T regulatory cells. *J Immunol*. Jul 1;179(1):154-61.
6. Chen X, Subleski JJ, Hamano R, Howard OM, Wiltrout RH, Oppenheim JJ.(2010) Co-expression of TNFR2 and CD25 identifies more of the functional CD4+FOXP3+ regulatory T cells in human peripheral blood. *Eur J Immunol*. Apr;40(4):1099-106.
7. Compston A, Coles A. (2008) Multiple sclerosis. *Lancet.* Oct 25;372(9648):1502-17.
8. Constantinescu CS, Farooqi N, O'Brien K, Gran B. (2011) Experimental autoimmune encephalomyelitis (EAE) as a model for multiple sclerosis (MS). *Br J Pharmacol.* Oct;164(4):1079-106.
9. Dendrou CA, Fugger L, Friese MA. (2015) Immunopathology of multiple sclerosis. *Nat Rev Immunol.* Sep 15;15(9):545-58.
10. Dong Y,Dekens D.W., De Deyn P.P., Naude P.J.W,, Eisel U.L.M (2015) Targeting of tumor necrosis factor alpha receptors as a therapeutic strategy for neurodegenerative disorders. *Antibodies*, 4(4), 369-408
11. Dong Y, Fischer R, Naudé PJ, Maier O, Nyakas C, Duffey M, Van der Zee EA, Dekens D, Douwenga W, Herrmann A, Guenzi E, Kontermann RE, Pfizenmaier K, Eisel UL. (2016) Essential protective role of tumor necrosis factor receptor 2 in neurodegeneration. *Proc Natl Acad Sci USA*. Oct 25;113(43):12304-12309.
12. EAE Induction by Active Immunization in C57BL/6 Mice. (2019, March 11). Retrieved November 03, 2020, from https://hookelabs.com/protocols/eaeAI_C57BL6.html
13. Eugster H.-P., Frei K., Bachmann R., Bluethmann H., Lassman H., Fontana A. (1999.) Severity of symptoms and demyelination in MOG induced EAE depends on TNFR1. *Immunology* 29:626-632
14. Fischer R., Padutsch T., Bracchi-Ricard V., Murphy K.L., Maritnez G.F., Delguercio N., Elmer N., Sendetski M., Diem R., Eisel U.L.M, Smeyne, R.J., Kontermann R.E., Pfizenmaier K., Bethea J.R.(2019) Exogenous activation of tumor necrosis factor receptor 2 promotes recovery from sensory and motor disease in a model of multiple sclerosis. *Brain, Behaviour and Immunity* 81: 247-259
15. Fischer R, Proske M, Duffey M, Stangl H, Martinez GF, Peters N, Kraske A, Straub RH, Bethea JR, Kontermann RE, Pfizenmaier K.(2018) Selective Activation of

Tumor Necrosis Factor Receptor II Induces Antiinflammatory Responses and Alleviates Experimental Arthritis. *Arthritis Rheumatol.* May;70(5):722-735.
16. Fischer R, Sendetski M, Del Rivero T, Martinez GF, Bracchi-Ricard V, Swanson KA, Pruzinsky EK, Delguercio N, Rosalino MJ, Padutsch T, Kontermann RE, Pfizenmaier K, Bethea JR. (2019) TNFR2 promotes Treg-mediated recovery from neuropathic pain across sexes. *Proc Natl Acad Sci U S A.* Aug 20;116(34):17045-17050.
17. Fischer R, Kontermann RE, Pfizenmaier K.(2020) Selective Targeting of TNF Receptors as a Novel Therapeutic Approach. *Front Cell Dev Biol*. May 26;8:401.
18. FlowJo™ Software for Windows [software application] Version 10. Ashland, OR: Becton, Dickinson and Company; 2019
19. FlowJo™ Software for Windows [DownSample algorithm] Version 10. Halpert R. 2019
https://docs.flowjo.com/seqgeq/dimensionality-reduction/downsample/
20. Fresegna D, Bullitta S, Musella A, Rizzo FR, De Vito F, Guadalupi L, Caioli S, Balletta S, Sanna K, Dolcetti E, Vanni V, Bruno A, Buttari F, Stampanoni Bassi M, Mandolesi G, Centonze D, Gentile A.(2020) Re-Examining the Role of TNF in MS Pathogenesis and Therapy. *Cells.* Oct 14;9(10):2290.
21. Friese MA, Fugger L.(2009) Pathogenic CD8(+) T cells in multiple sclerosis. *Ann Neurol*. Aug;66(2):132-41.
22. Gravano DM, Hoyer KK.(2013) Promotion and prevention of autoimmune disease by CD8+ T cells. *J Autoimmun.*Sep;45:68-79
23. Howard J, Trevick S, Younger DS.(2016) Epidemiology of Multiple Sclerosis. *Neurol Clin.* Nov;34(4):919-939.
24. Van Kaer L, Postoak JL, Wang C, Yang G, Wu L.(2019) Innate, innate-like and adaptive lymphocytes in the pathogenesis of MS and EAE. *Cell Mol Immunol*. Jun;16(6):531-539.
25. Kaltsonoudis E, Voulgari PV, Konitsiotis S, Drosos AA. (2014) Demyelination and other neurological adverse events after anti-TNF therapy. *Autoimmun Rev.* Jan;13(1):54-8.
26. Kaskow BJ, Baecher-Allan C.(2018) Effector T Cells in Multiple Sclerosis. *Cold Spring Harb Perspect Med.* Apr 2;8(4):a029025.
27. Kruglov AA, Lampropoulou V, Fillatreau S, Nedospasov SA. (2011)Pathogenic and protective functions of TNF in neuroinflammation are defined by its expression in T lymphocytes and myeloid cells. *J Immunol.* Dec 1;187(11):5660-70.
28. Joep Killestein, M.Judith Eikelenboom, Thijs Izeboud, Nynke F. Kalkers, Herman J. Adèr, Frederik Barkhof, Rene A.W. Van Lier, Bernard M.J. Uitdehaag, Chris H. Polman (2000),Cytokine producing CD8+ T cells are correlated to MRI features of tissue destruction in MS, *Journal of Neuroimmunology*, Volume 142, Issues 1–2,141-148
29. Lassmann H, Bradl M. (2017) Multiple sclerosis: experimental models and reality. *Acta Neuropathol*.Feb;133(2):223-244.
30. Lee HW, Gangadaran P, Kalimuthu S, Ahn BC. (2016) Advances in Molecular Imaging Strategies for In Vivo Tracking of Immune Cells. *Biomed Res Int*:1946585.
31. Maddur MS, Miossec P, Kaveri SV, Bayry J.(2012) Th17 cells: biology, pathogenesis of autoimmune and inflammatory diseases, and therapeutic strategies. *Am J Pathol*. Jul;181(1):8-18.

32. Miller PG, Bonn MB, McKarns SC. (2015) Transmembrane TNF-TNFR2 Impairs Th17 Differentiation by Promoting Il2 Expression. *J Immunol.* Sep 15;195(6):2633-47.
33. Monaco G, Chen H, Poidinger M, Chen J, de Magalhaes JP, Larbi A.:(2016) flowAI: automatic and intercative anomaly discerning tools for flow cytometry data. *Bioinformatics* Aug 15, 32(16): 2473-80
34. Nie H, Zheng Y, Li R, Zhang J. (2016)Reply to Suppressive activity of human regulatory T cells is maintained in the presence of TNF. *Nat Med.*Jan;22(1):18-9.
35. O'Connor RA, Prendergast CT, Sabatos CA, Lau CW, Leech MD, Wraith DC, Anderton SM. (2008) Cutting edge: Th1 cells facilitate the entry of Th17 cells to the central nervous system during experimental autoimmune encephalomyelitis. *J Immunol*. Sep 15;181(6):3750-4.
36. Paintlia AS, Paintlia MK, Singh I, Singh AK. (2006) IL-4-induced peroxisome proliferator-activated receptor gamma activation inhibits NF-kappaB trans activation in central nervous system (CNS) glial cells and protects oligodendrocyte progenitors under neuroinflammatory disease conditions: implication for CNS-demyelinating diseases. *J Immunol.*Apr 1;176(7):4385-98.
37. Peng Y, Zhu FZ, Chen ZX, Zhou JX, Gan L, Yang SS, Gao S, Liu QQ. (2019) Characterization of myelin oligodendrocyte glycoprotein (MOG)35-55-specific CD8+ T cells in experimental autoimmune encephalomyelitis. *Chin Med J (Engl)*. Dec 20;132(24):2934-2940.
38. Pegoretti V, Baron W, Laman JD, Eisel ULM. (2018) Selective Modulation of TNF-TNFRs Signaling: Insights for Multiple Sclerosis Treatment. *Front Immunol.*Apr 30;9:925.
39. Probert L. (2015) TNF and its receptors in the CNS: The essential, the desirable and the deleterious effects. *Neuroscience*. Aug 27;302:2-22.
40. Richter F, Seifert O, Herrmann A, Pfizenmaier K, Kontermann RE. (2019) Improved monovalent TNF receptor 1-selective inhibitor with novel heterodimerizing Fc. MAbs. May/Jun;11(4):653-665.
41. Sharief MK, Hentges R. (1991) Association between tumor necrosis factor-alpha and disease progression in patients with multiple sclerosis. *N Engl J Med*. Aug 15;325(7):467-72.
42. Sinha S, Boyden AW, Itani FR, Crawford MP, Karandikar NJ. (2015) CD8(+) T-Cells as Immune Regulators of Multiple Sclerosis. *Front Immunol.*Dec 10;6:619
43. Taoufik E, Tseveleki V, Chu SY, Tselios T, Karin M, Lassmann H, Szymkowski DE, Probert L. (2011) Transmembrane tumour necrosis factor is neuroprotective and regulates experimental autoimmune encephalomyelitis via neuronal nuclear factor-kappaB. *Brain.* 134(Pt 9):2722-35.
44. Thakker P, Leach MW, Kuang W, Benoit SE, Leonard JP, Marusic S. (2007) IL-23 is critical in the induction but not in the effector phase of experimental autoimmune encephalomyelitis. *J Immunol*.Feb 15;178(4):2589-98.
45. The Lenercept Multiple Sclerosis Study Group and The University of British Columbia MS/MRI Analysis Group. (1999) TNF neutralization in MS: results of a randomized, placebo-controlled multicenter study. *Neurology* 53: 457–465.
46. Trapp B.D., Nave K.A. (2008) Multiple sclerosis: An Immune or Neurodegenerative Disorder? *Annu.Rev.Neurosci*. 31:247-269

47. Vaisman-Mentesh A, Rosenstein S, Yavzori M, Dror Y, Fudim E, Ungar B, Kopylov U, Picard O, Kigel A, Ben-Horin S, Benhar I, Wine Y (2019). Molecular Landscape of Anti-Drug Antibodies Reveals the Mechanism of the Immune Response Following Treatment With TNFα Antagonists. *Front Immunol.* Dec 18;10:2921.
48. Van Gassen S, Callebaut B, Van Helden MJ, Lambrecht BN, Demeester P, Dhaene T, Saeys Y. (2015) FlowSOM: Using self-organizing maps for visualization and interpretation of cytometry data. *Cytometry A.* Jul;87(7):636-45.
49. Whitacre C. (2004) Spotlight on CD8 T cells in MS. *Blood* 103(11): 3999-4000
50. Yang S, Wang J, Brand DD, Zheng SG. (2018) Role of TNF-TNF Receptor 2 Signal in Regulatory T Cells and Its Therapeutic Implications. *Front Immunol*. Apr 19;9:784
51. Ye LL, Wei XS, Zhang M, Niu YR, Zhou Q. (2018) The Significance of Tumor Necrosis Factor Receptor Type II in CD8+ Regulatory T Cells and CD8+ Effector T Cells. *Front Immunol.*Mar 22;9:583.
52. Williams SK, Maier O, Fischer R, Fairless R, Hochmeister S, Stojic A, Pick L, Haar D, Musiol S, Storch MK, Pfizenmaier K, Diem R. (2014) Antibody-mediated inhibition of TNFR1 attenuates disease in a mouse model of multiple sclerosis. *PLoS One.* Feb 28;9(2):e90117.
53. Williams SK, Fairless R, Maier O, Liermann PC, Pichi K, Fischer R, Eisel ULM, Kontermann R, Herrmann A, Weksler B, Romero N, Couraud PO, Pfizenmaier K, Diem R. (2018) Anti-TNFR1 targeting in humanized mice ameliorates disease in a model of multiple sclerosis. *Sci Rep*Sep 11;8(1):13628.
54. Zhang L, Jarvis LB, Baek HJ, Gaston JS. (2009) Regulatory IL4+CD8+ T cells in patients with ankylosing spondylitis and healthy controls. *Ann Rheum Dis.* Aug;68(8):1345-51.

Appendix 1:

Table explaining the criteria of clinical scoring during EAE observation:

<table>
<tr><th>Clinical score</th><th>Symptom description</th><th>Sub-score</th><th>Symptom description</th></tr>
<tr><td rowspan="3">0</td><td rowspan="3">No obvious symptoms. The tail has tension and the tip of the tail can curl.</td><td>.25</td><td>Tip of the tail is limp.</td></tr>
<tr><td>.5</td><td>Half of the tail is limp, but there is tension and movement of the rest of the tail.</td></tr>
<tr><td>.75</td><td>Most of the tail is limp, but it is not hanging.</td></tr>
<tr><td rowspan="3">1</td><td rowspan="3">The whole tail is limp and there is no tension. The animal's movement is normal.</td><td>.25</td><td>Walking might be wobbly.When put on the cage grid, the legs are mostly not falling.</td></tr>
<tr><td>.5</td><td>Walking is wobbly.When put on the cage grid, at least one leg falls through consistently.</td></tr>
<tr><td>.75</td><td>Walking is wobbly. One or both legs fall through more than half of the time.</td></tr>
<tr><td rowspan="3">2</td><td rowspan="3">The whole tail is limp and there are obvious signs of weakness and movement issues in the hind legs.</td><td>.25</td><td>Hind legs are not underneath the body anymore.</td></tr>
<tr><td>.5</td><td>One or both feet are dragging, but there is some movement in them.</td></tr>
<tr><td>.75</td><td>Both legs are dragging, they hang away from the body, but there is still some movement.</td></tr>
<tr><td>3</td><td>The whole tail is limp and the hind legs are paralyzed. The animal is dragging the hind legs on the side.</td><td colspan="2" rowspan="3">Animals in this experiment did not exceed the score of 3. The relatively mild course of EAE was expected. If any animal had reached the score of 4 or 5 it would have been sacrificed.</td></tr>
<tr><td>4</td><td>The whole tail is limp, hind legs are paralyzed and the front limbs are partially paralyzed.</td></tr>
<tr><td>5</td><td>Severe paralysis.</td></tr>
</table>

Appendix 2:

Figure 1. Represented are all steps in the manual gating procedure, from the FlowAI algorithm to the separation of IL-17+ and IFNγ+ cells in the CD4+ population. The figure was produced by FlowJo.

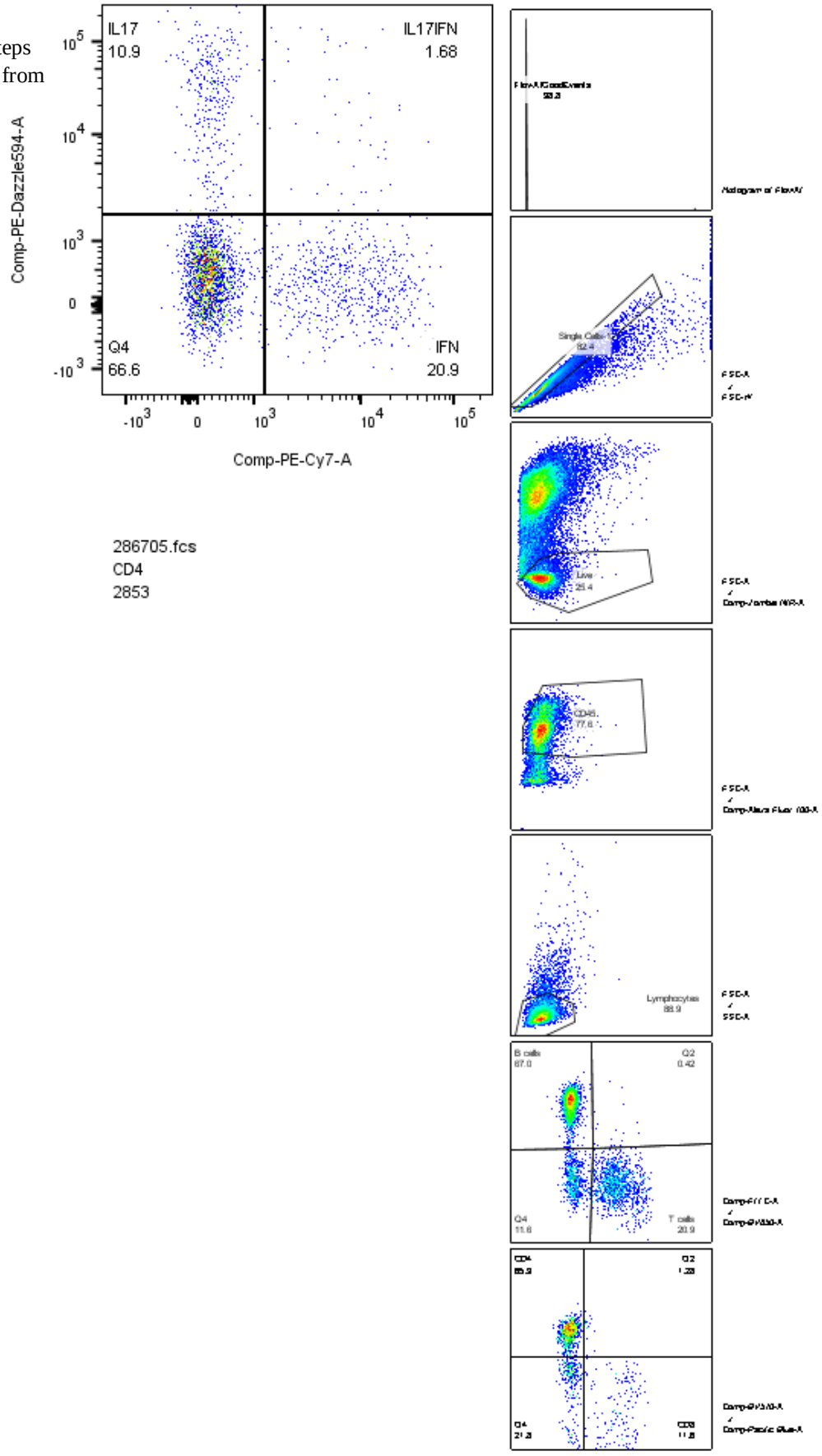

Appendix 3:

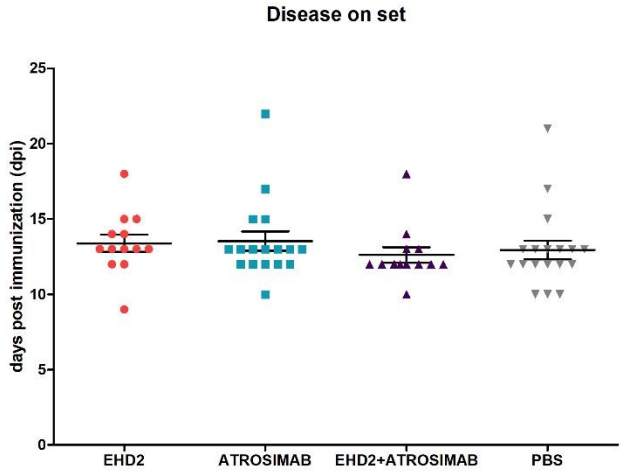

Figure 1. No significant difference was found in disease onset. Most animals developed disease between days 9 to 14. Some developed symptoms later. Dots on the x-axis represent the animals that did not develop the disease until day 18 or 25. Animals on the graph are from the acute and chronic group. Day of disease onset is presented as mean± SEM. No significance was detected by Kruskal-Wallis or Man-Whitney tests.

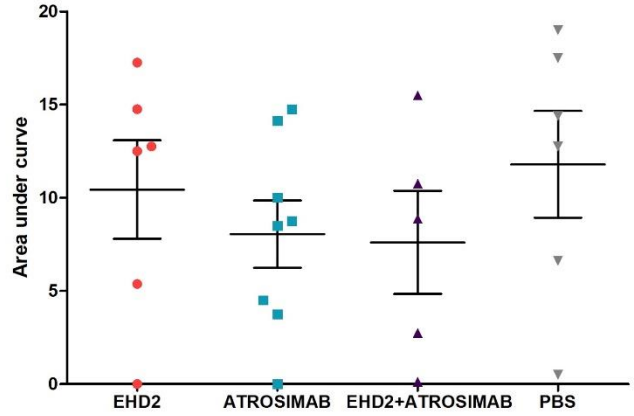

Figure 2. Animals from the acute phase had no differences in cumulative scores across treatments. Cumulative score presented as mean ± SEM of areas under the disease curve. No significance was detected by Kruskal-Wallis or Man-Whitney tests.

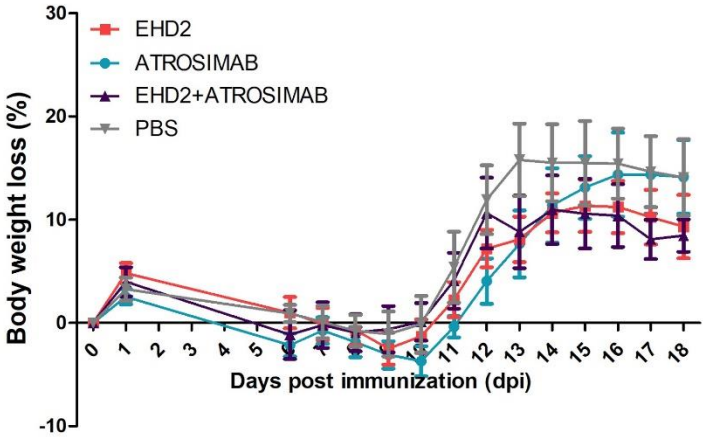

Figure 3. After immunization animals initially lose weight, but stay relatively stable, until the disease onset. During the increase of the clinical scores, the body weight starts to drop. Body weight loss is calculated in relation to day 0 post-immunization and is presented as mean ± SEM. No significance was detected by Kruskal-Wallis or Man-Whitney tests.

Appendix 4:

Table of excluded animals based on premature death:

Treatment group	EAE number	Exclusion criteria
EHD2	1	Died 25 minutes after the third injection due to a shock-like reaction. (12 dpi)
EHD2	23	Found dead due to high EAE score and low body weight. (15 dpi)
PBS	26	Humane end-point due to low body weight. (14 dpi)
EHD2+ATROSIMAB	28	Died 25 minutes after the third injection due to a shock-like reaction.(12 dpi)
EHD2+ATROSIMAB	32	Found dead due to high EAE score and low body weight. (15 dpi)
EHD2+ATROSIMAB	46	Died 25 minutes after the third injection due to a shock-like reaction.(12 dpi)
EHD2	54	Died 25 minutes after the third injection due to a shock-like reaction.(12 dpi)
EHD2+ATROSIMAB	55	Died 25 minutes after the third injection due to a shock-like reaction.(12 dpi)
EHD2+ATROSIMAB	59	Died 25 minutes after the third injection due to a shock-like reaction.(12 dpi)
EHD2+ATROSIMAB	62	Died 25 minutes after the third injection due to a shock-like reaction.(12 dpi)
EHD2	66	Died 25 minutes after the third injection due to a shock-like reaction.(12 dpi)
EHD2	72	Died 25 minutes after the third injection due to a shock-like reaction.(12 dpi)
EHD2+ATROSIMAB	75	Died 25 minutes after the third injection due to a shock-like reaction.(12 dpi)
EHD2+ATROSIMAB	79	Died 25 minutes after the third injection due to a shock-like reaction.(12 dpi)

Treatment	Number of animals in the <u>acute</u> group:	Number of animals that did not develop EAE:	Disease incidence:
EHD2	6	1	83.3%
ATROSIMAB	7	1	86%
EHD2+ ATROSIMAB	5	1	80%
PBS	6	1	83.3%

Appendix 5:

FlowSOM graphs: (trees presented in the results section, also included here, highlighted)

MST tree of T cell subsets in the spleens of the EHD2 group (acute):

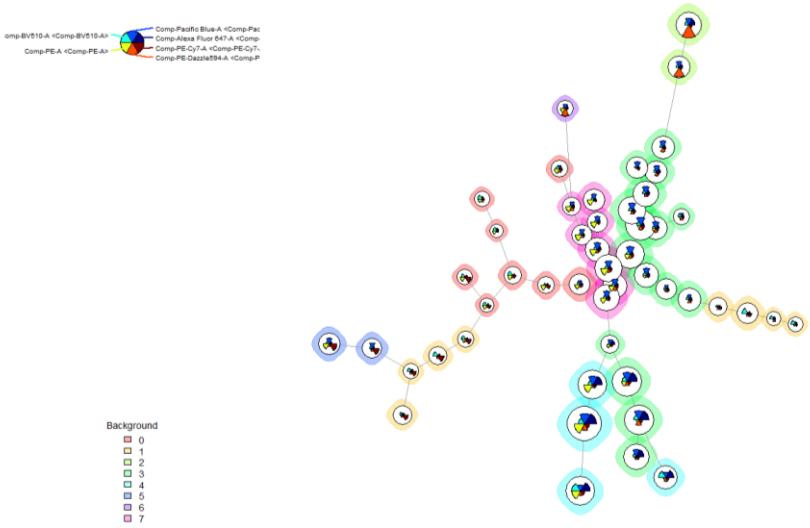

MST tree of T cell subsets in the spleens of the ATROSIMAB group (acute):

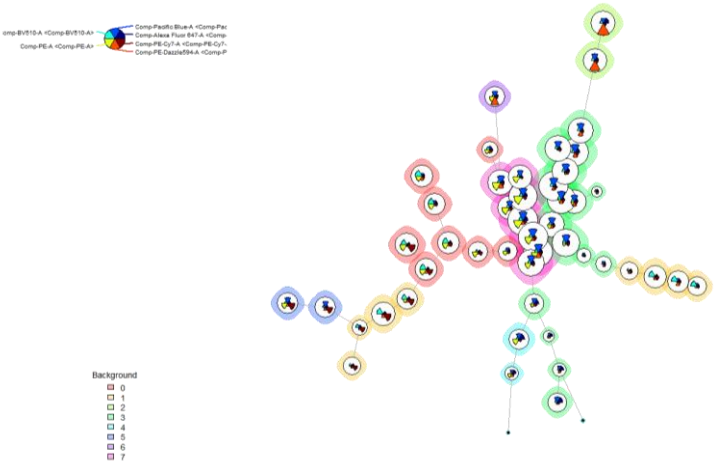

MST tree of T cell subsets in the spleens of the combination group (acute):

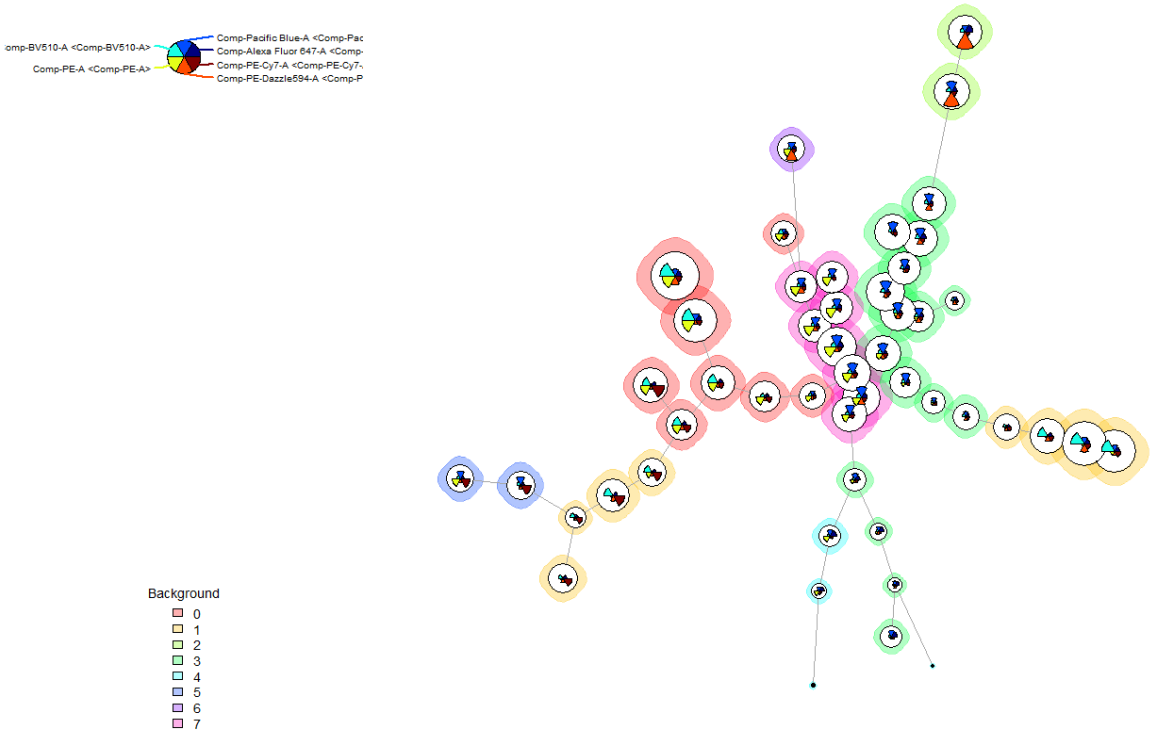

MST tree of T cell subsets in the spleens of the PBS group (acute):

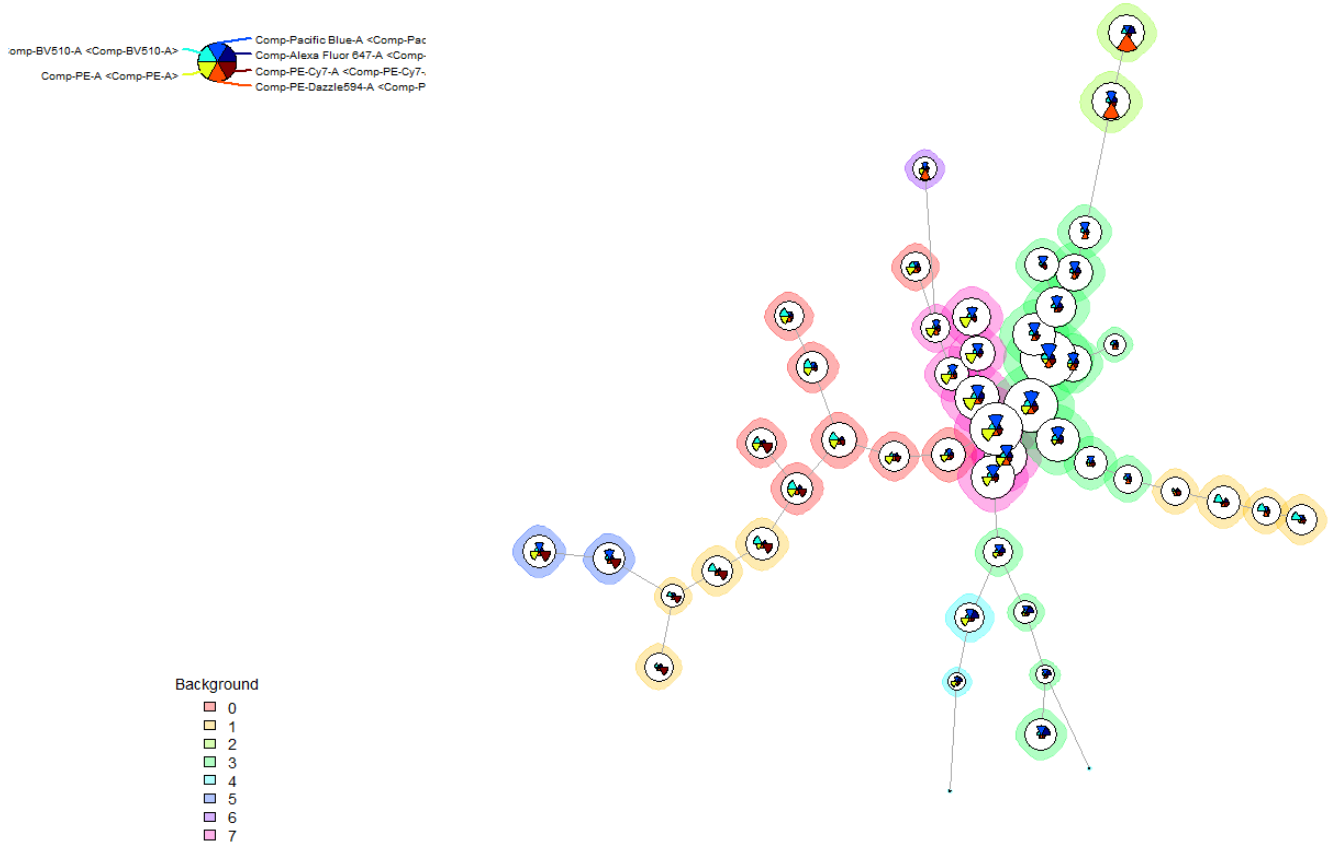

MST tree of T cells in the spleen of the EHD2 group (chronic):

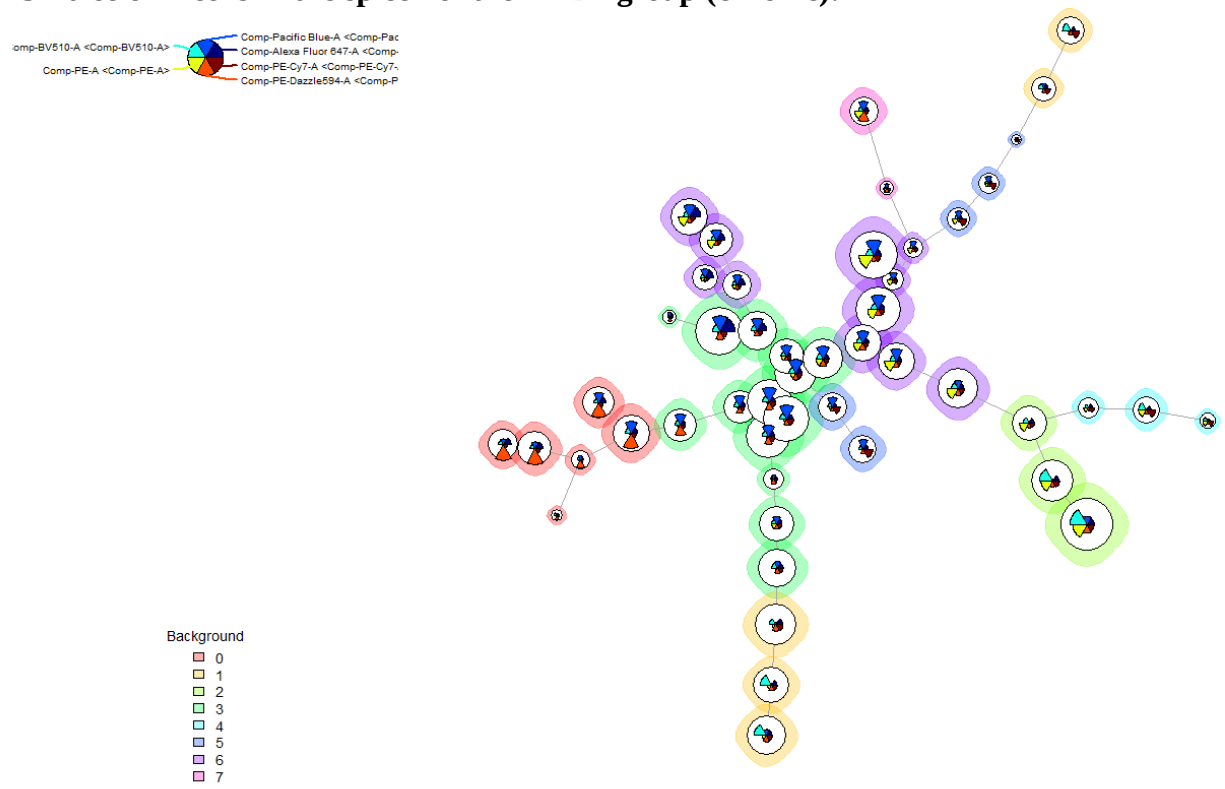

MST of the cells in the spleen of the ATROSIMAB group (chronic stage):

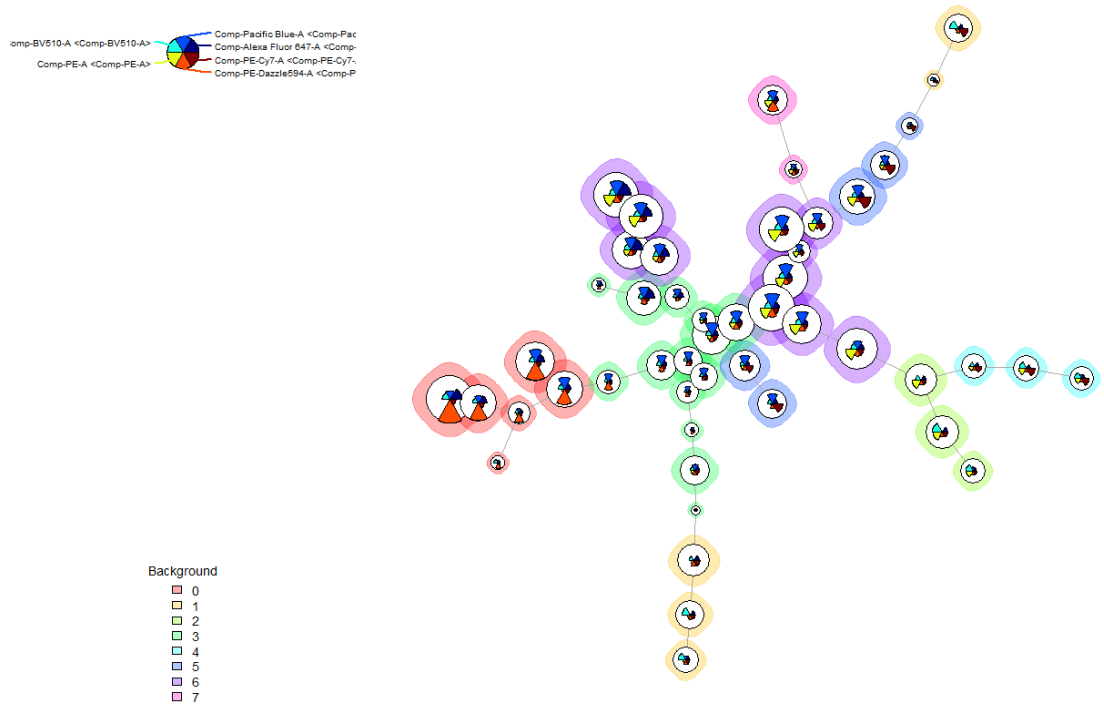

MST of the cells in the spleen of the combiantion group (Chronic):

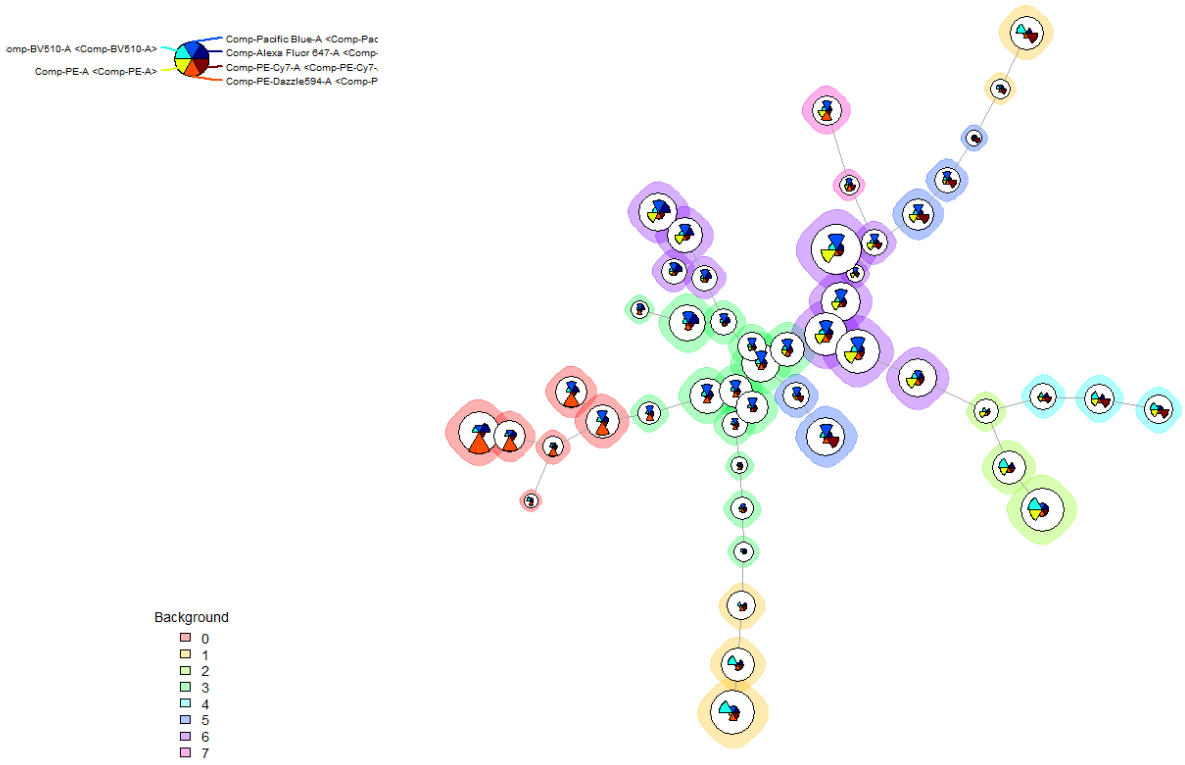

FlowSOM of the cells in the spleen of the PBS group (chronic):

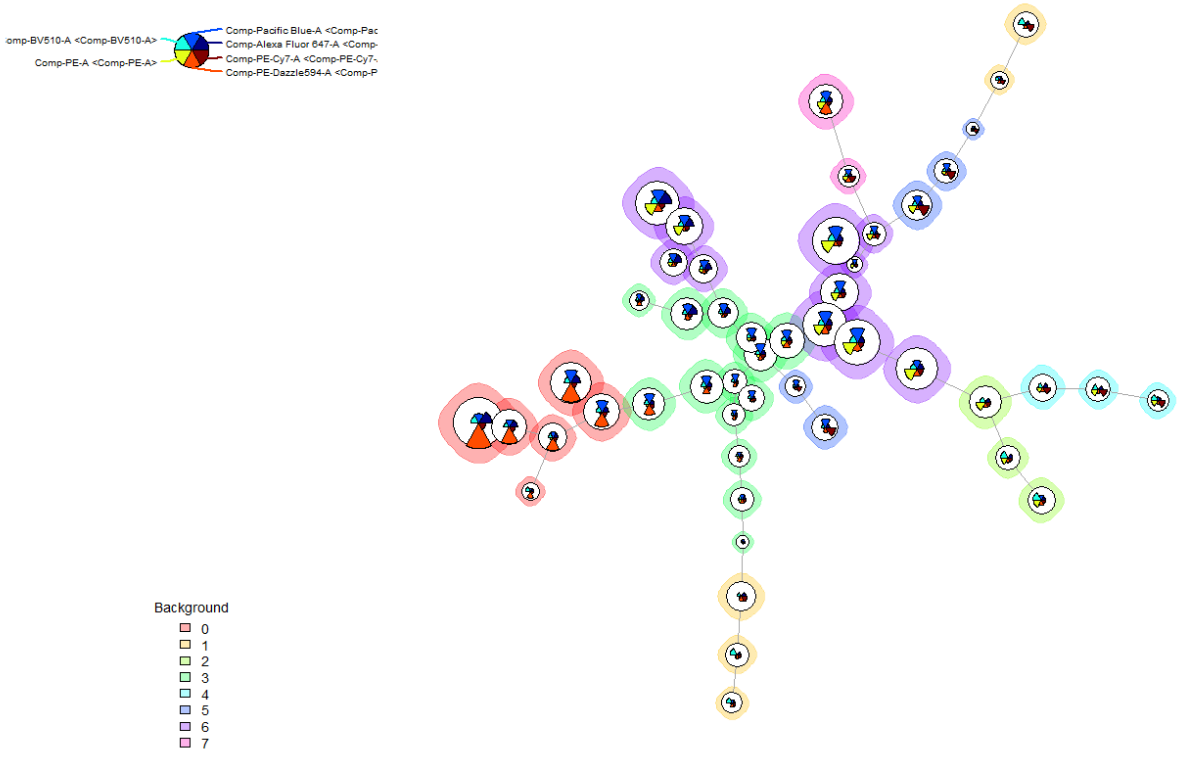

MST tree of T cell subsets in the lymph nodes of the EHD2 group (acute):

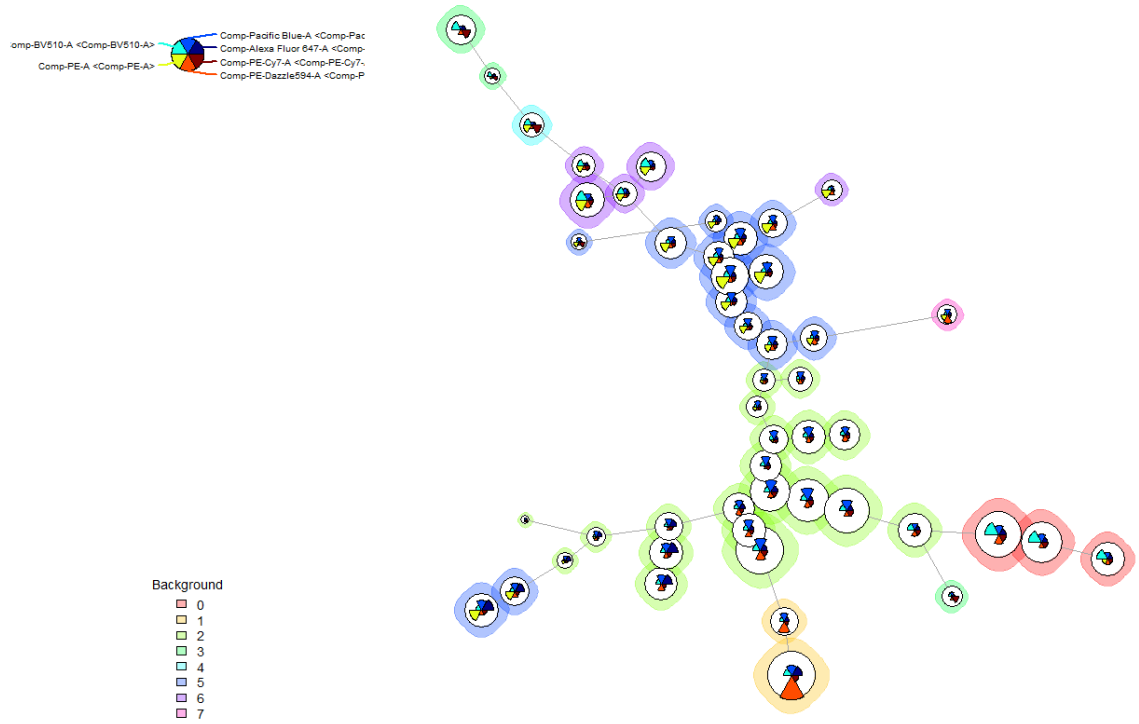

MST tree of T cell subsets in the lymph nodes of the ATROSIMAB group (acute):

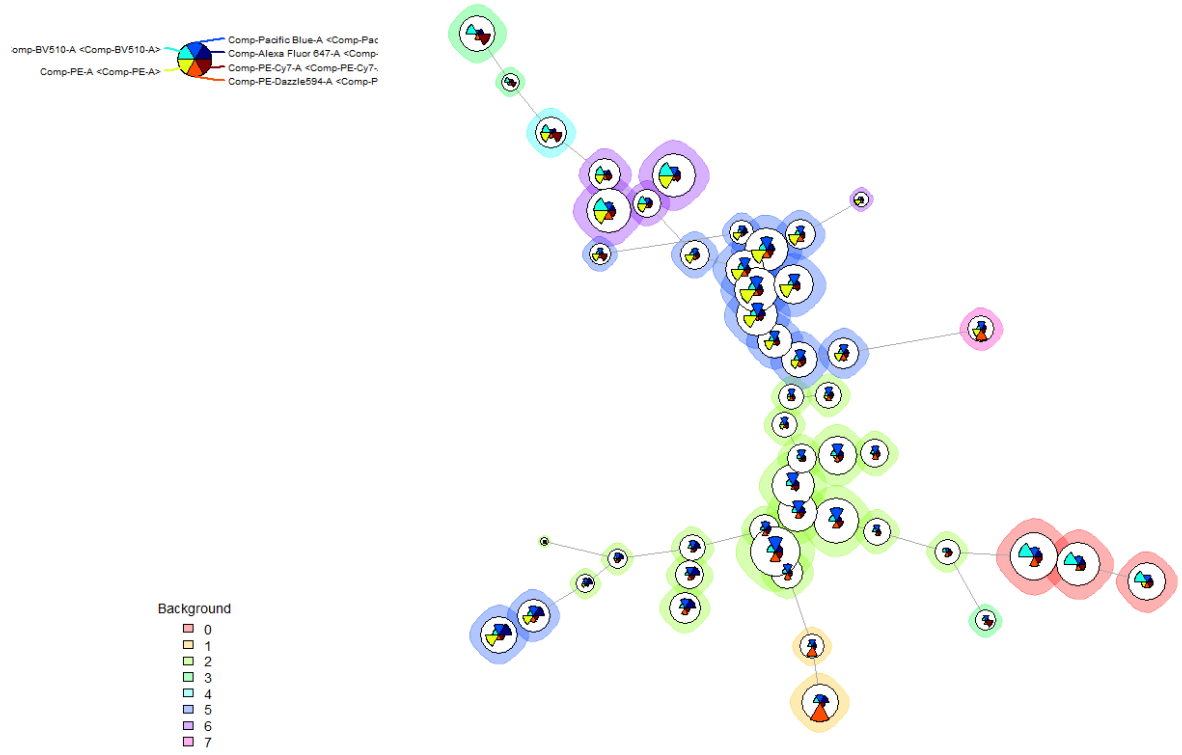

MST tree of T cell subsets in the lymph nodes of the combination group (acute):

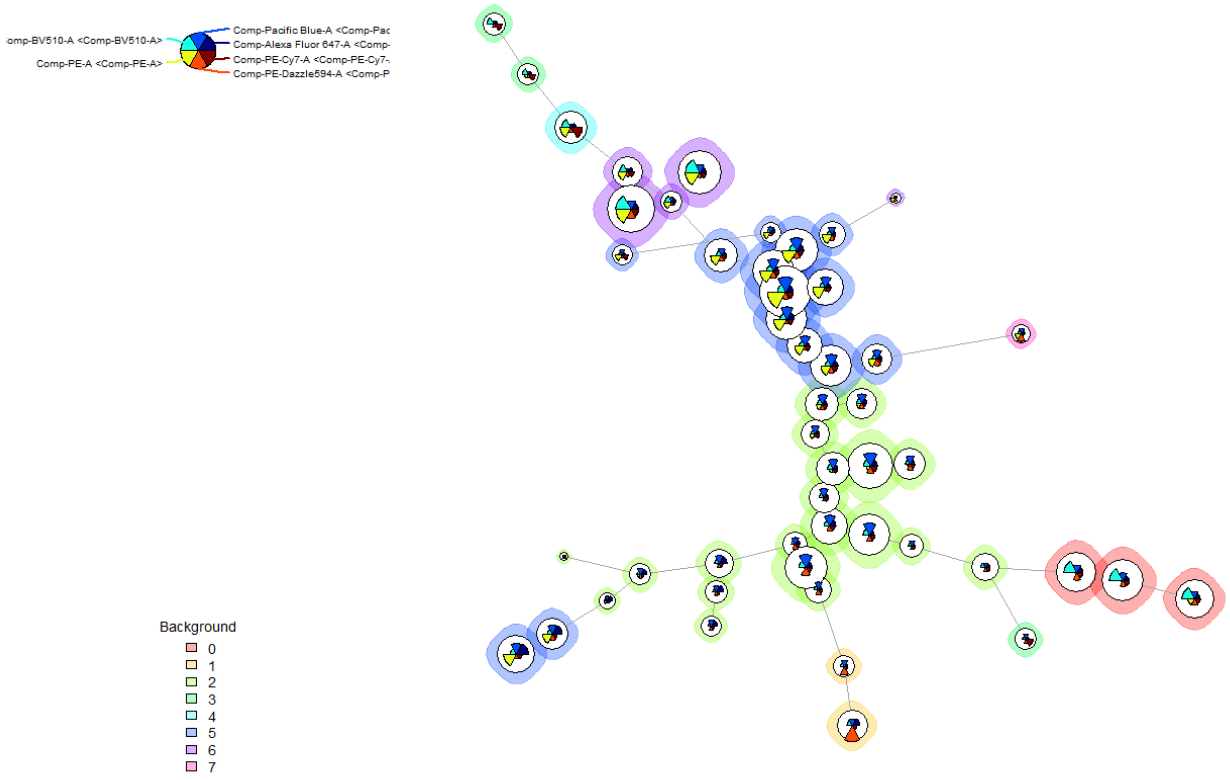

MST tree of T cell subsets in the lymph nodes of the PBS group (acute):

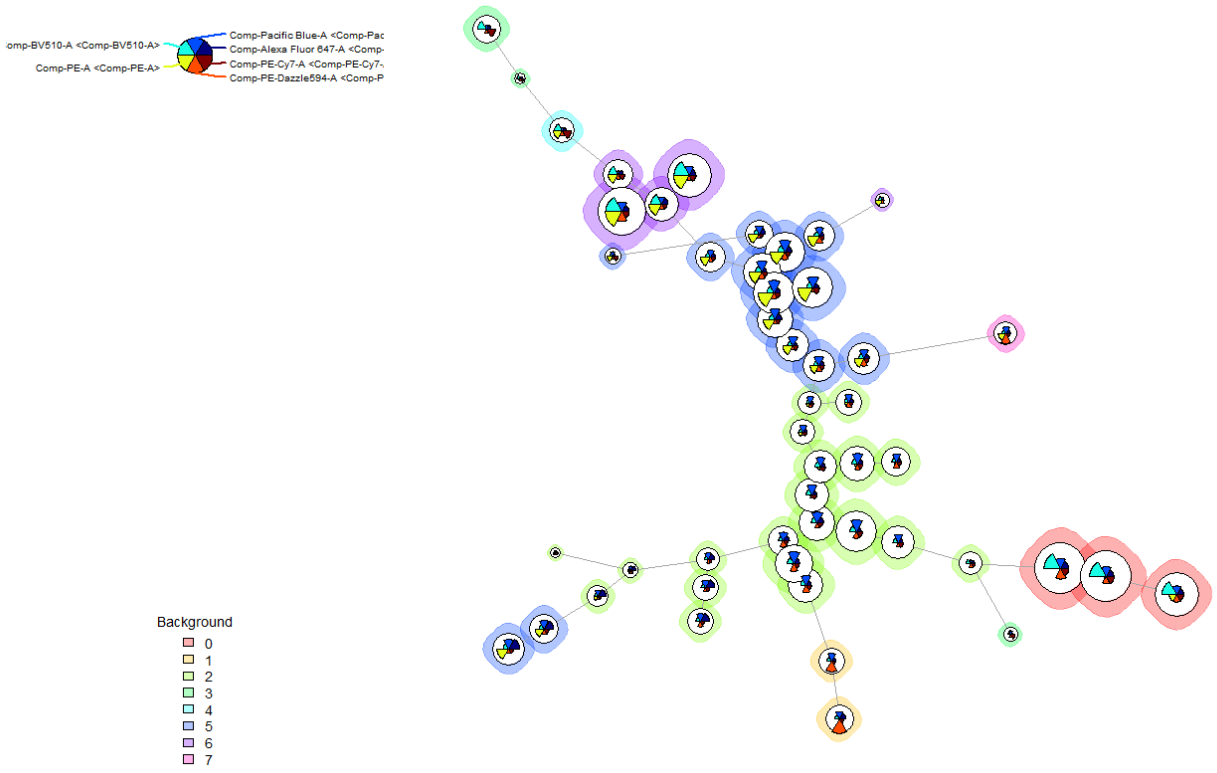

MST tree of T cell subsets in the lymph nodes of the EHD2 group (chronic):

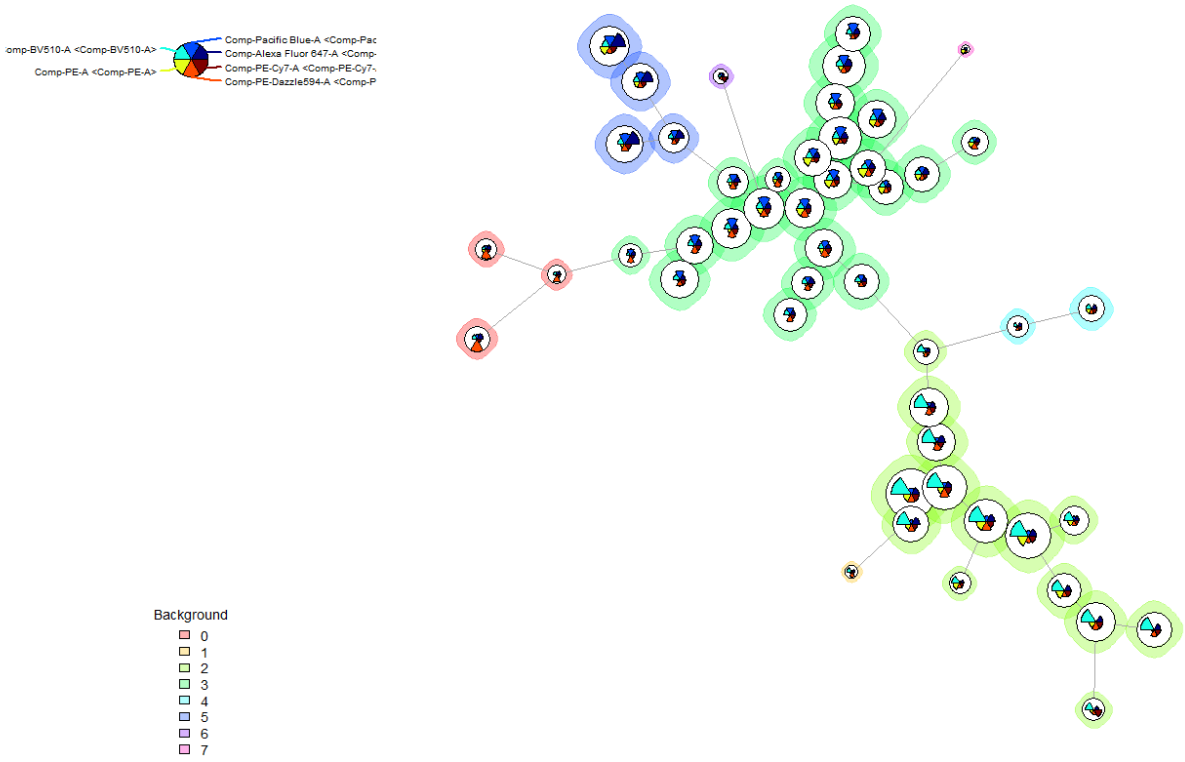

MST tree of T cell subsets in the lymph nodes of the ATROSIMAB group (chronic):

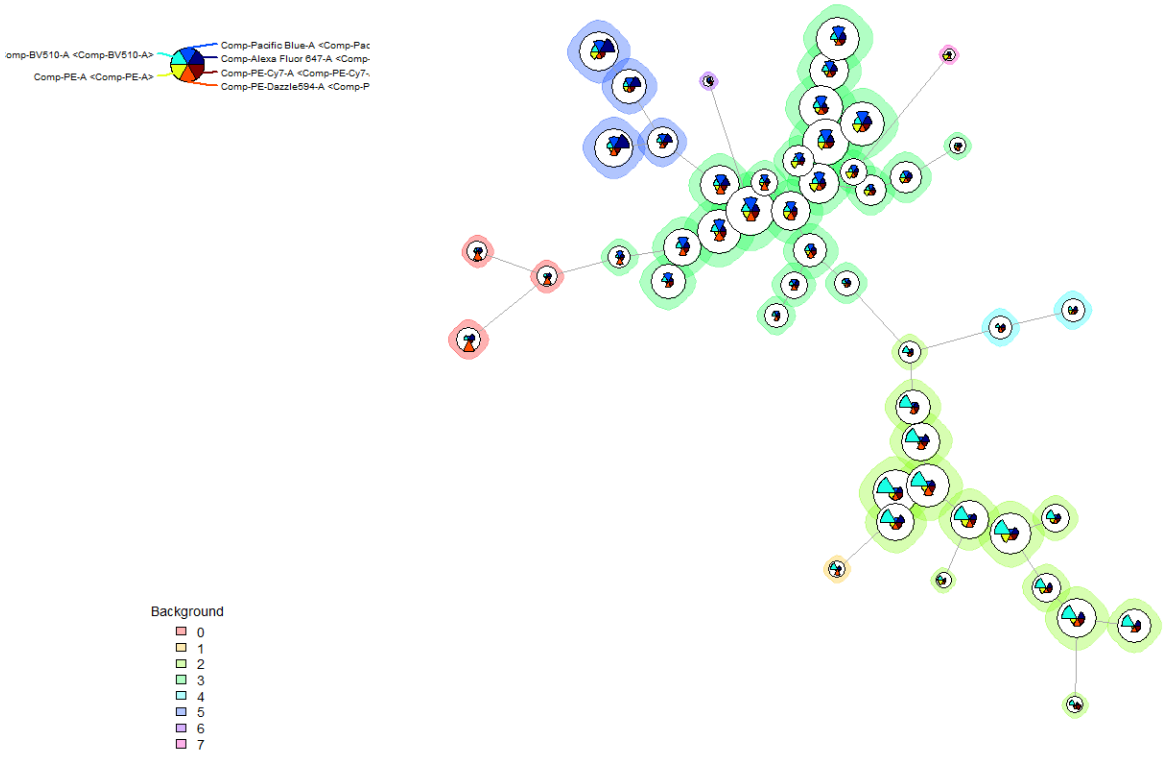

MST tree of T cell subsets in the lymph nodes of the combination group (chronic):

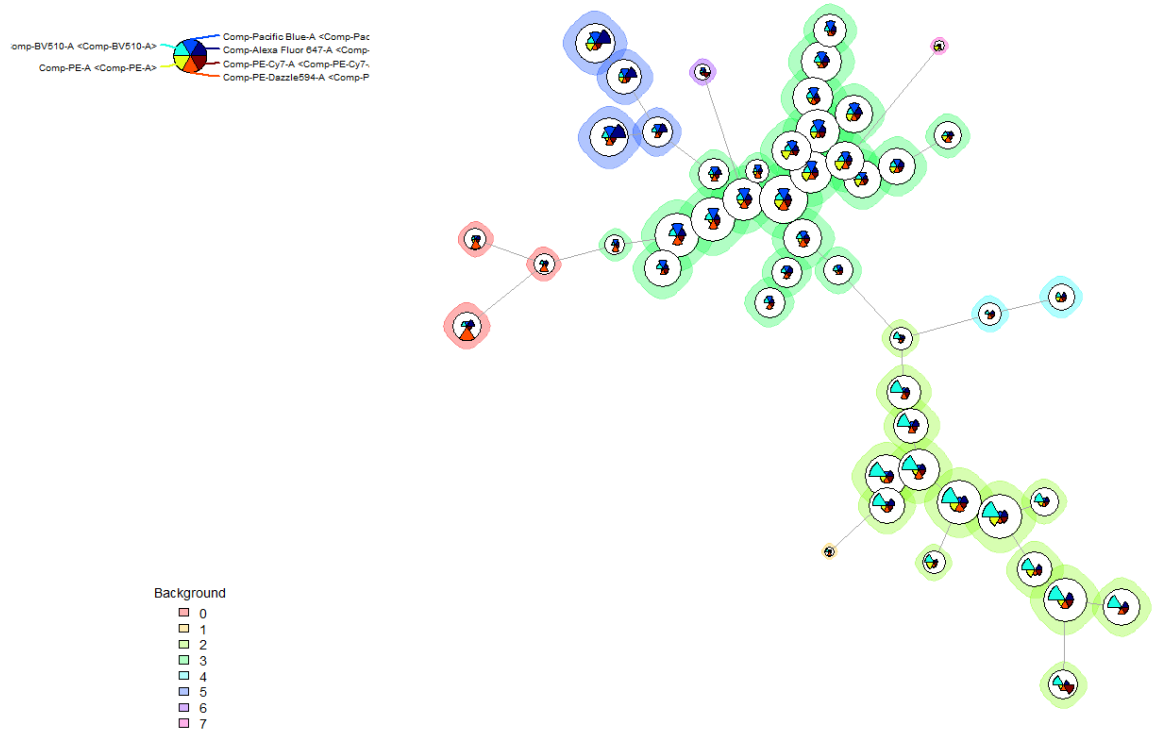

MST tree of T cell subsets in the lymph nodes of the PBS group (chronic):